Journal Pre-proof

Mode-switching cooperative defense strategy for the Orbit Pursuit-Evasion-Defense Game

Yongshang Wei, Tianxi Liu, Cheng Wei

PII: S2214-9147(24)00249-6

DOI: https://doi.org/10.1016/j.dt.2024.10.006

Reference: DT 1523

To appear in: *Defence Technology*

Received Date: 23 July 2024

Revised Date: 9 September 2024

Accepted Date: 22 October 2024

Please cite this article as: Wei Y, Liu T, Wei C, Mode-switching cooperative defense strategy for the Orbit Pursuit-Evasion-Defense Game, *Defence Technology*, https://doi.org/10.1016/j.dt.2024.10.006.

Mode-switching cooperative defense strategy for the Orbit Pursuit-Evasion-Defense Game

Yongshang Wei[a], Tianxi Liu[a,*], Cheng Wei[a]

[a]School of aerospace, Harbin Institute of Technology, Harbin 150000, China

[*]Corresponding author: liutianxi@hit.edu.cn.

Mode-switching cooperative defense strategy for the Orbit Pursuit-Evasion-Defense Game

Abstract

This paper presents a mode-switching collaborative defense strategy for spacecraft pursuit-evasion-defense scenarios. In these scenarios, the pursuer tries to avoid the defender while capturing the evader, while the evader and defender form an alliance to prevent the pursuer from achieving its goal. First, the behavioral modes of the pursuer, including attack and avoidance modes, were established using differential game theory. These modes are then recognized by an interactive multiple model-matching algorithm (IMM), that uses several smooth variable structure filters to match the modes of the pursuer and update their probabilities in real time. Based on the linear-quadratic optimization theory, combined with the results of strategy identification, a two-way cooperative optimal strategy for the defender and evader is proposed, where the evader aids the defender to intercept the pursuer by performing luring maneuvers. Simulation results show that the interactive multi-model algorithm based on several smooth variable structure filters perform well in the strategy identification of the pursuer, and the cooperative defense strategy based on strategy identification has good interception performance when facing pursuers, who are able to flexibly adjust their game objectives.

Keywords：Cooperative policy； Differential games; Orbit pursuit-evasion-defense game; Mod recognition

1. Introduction

The pursuit-evasion game has received considerable attention from researchers because it fits the characteristics of many practical problems and the related theories and applications have made significant progress in recent decades. As human activities in space intensify, the number of man-made objects and assets in space has increased dramatically; therefore, issues such as on-orbit maintenance, space debris removal, and collision avoidance are receiving increased attention [1-3]. The pursuit-evasion game is a theoretical tool for studying these areas.

The spacecraft orbit pursuit-evasion game (OPEG) has garnered immense attention from scholars over the past half century and many results have been achieved. OPEG research can be divided into long-distance orbital pursuit-evasion games (LDOPEGs) and short-distance orbital pursuit-evasion games (SDOPEGs). Because of the complex high-dimensional nonlinear dynamics of the LDOPEG, scholars have mainly focused on researching fast, computationally light-loaded, and robust numerical solution methods. For example, Pontani and Conway [4] expressed the optimal control of one party in the form of its state and covariate variables through the optimality necessity condition and solved the transformed optimal control problem using a semi-directive collocation-point nonlinear programming method to obtain LDOPEG. Zeng and Yang et al. [5] solved the LDOPEG in the Cartesian and spherical coordinate systems, respectively, solved the two-point boundary value problem obtained from the optimality necessity condition using a mixed global-local optimization strategy, and analyzed the results in the two coordinate systems. Hafer and Reed [6] applied the sensitivity method to the solution of the OPEG to improve its efficiency by constructing and tracking homotopy trajectories from zero gravity to full gravity. Ye et al. [7,8] investigated the OPEG in the cases where the thrust direction was restricted and where the pursuer adopted a three-axis thrust configuration, and solved them using numerical methods. Similar results have been previously reported [9-11]. With respect to SDOPEG, scholars have focused on optimal or near-optimal strategies with better robustness that can satisfy real-time requirements. For example, Zhang et al. [12] proposed a near-optimal pursuit strategy based on deep learning inside the capture zone of an OPEG, whereas a reinforcement learning-based capture zone embedding strategy was proposed outside the capture zone such that the state crosses the barrier into the capture zone. Ye et al. [13] proposed a pursuit guidance law that can be computed quickly based on differential game theory by numerically solving a nonlinear integral equation to define the end-of-game moment, and used it to compute the zero-effort-miss (ZEM) to obtain the optimal guidance law. Tang et al. [14] designed a pursuit guidance law using linear quadratic differential game theory. They considered the unavailability of the evader's evaluation function by designing an interactive multi-model matching algorithm to recognize its escape pattern and therefore match the optimal guidance law. Inspired by the predatory behavior of dragonflies, Li et al. [15] proposed a covert pursuit strategy that forces the pursuer to remain in line between the central spacecraft and the evader to continue approaching the evader for achieving covert purpose. Dan Shen and Bin Jia et al. [16] considered the spatial situational awareness problem, and designed the game between the pursuer and evader about the orbital uncertainty. In addition to orbital games, many other types of games have been studied in literatures. For example, Vinodhini Comandur and Tulasi Ram Vechalapu et al. [17] studied the game under asymmetric information and designed desensitization strategy and deception strategy for the pursuer and evader respectively. Asgharnia and Schwartz et al. [18] studied territorial defense in a grid world and designed a deception strategy using a machine learning method. The method is designed in two layers, the first layer generates a strategy for the identified territory, and the second layer determines which territory to invade. Tulasi Ram Vechalapu [19] proposed a pursuit strategy for a high speed evader, in which multiple pursuers cooperate to trap and capture the evader.

In the aforementioned studies, the evader often used its own maneuvering strategy to evade the pursuer. In such scenarios, the evader is required to have a certain degree of maneuverability and carry extra fuel. As the evader continues to maneuver, it will continue to deviate from its original mission trajectory, thereby affecting the original mission. Recently, several scholars study game scenarios where a defender exists, to address the threat of an orbiting spacecraft facing the pursuer. The defender aims to capture or dislodge the pursuer before the pursuer captures the evader, thereby safeguarding the evader's original mission. Israeli scientists have demonstrated this through missile guidance. Tal Shima [20] designed an optimal coordinated defense strategy using the defender's terminal zero-effort-miss as an evaluation function under the assumption that the pursuer adopts a known linear guidance law. Here, the evader lures the pursuer into the defender's collision path using its own maneuvering, which achieves coordination. Furthermore, assuming that the pursuer guidance law is known, Weiss and Shima [21] used fuel consumption as an evaluation function and the zero-effort-miss between the pursuer and evader and between the defender and pursuer as constraints, and ultimately devised minimum-effort intercept and evasion strategies with respect to a generalized dead-band function. Perelman and Shima [22] solved the differential game problem for the pursuer and defense teams using a linear dynamics model with a quadratic performance index comprising terminal states and control integrals, relaxing the assumption that the pursuer's strategy is known. Li and Wang et al. [23] designed a collaborative defense strategy in terms of unilateral and bidirectional collaboration using the defender's zero-effort-miss as a constraint and energy consumption as an evaluation function. However, this strategy requires knowledge of the pursuer's instantaneous acceleration and the assumption that the pursuer adopts a constant strategy for one guidance cycle. Liang and Wang et al. [24] studied a two-on-two game process in which the evader and defender is a team and the pursuer and protector is the other team. They proposed two strategies based on a norm-based performance index and a linear quadratic-based performance index. The aforementioned studies obtained results in the context of linearizing the dynamic model near the collision path in the missile terminal guidance phase. There are many other results related to cooperative defense with respect to simple motion models [25-29], most of which are based on a geometric approach to analyze the respective winning regions of the two sides of the game and then obtain the complete solution of the game on this basis.

In the spacecraft active defense field, where the results are not as abundant as those in the field of missile guidance rate design, Liu et al. [30] investigated an on-orbit three-member defense problem and proposed a hybrid approach that combines particle swarm optimization with Newtonian iteration. In addition to active defense techniques, there are pursuit strategies that consider evading defenders, such as those in the work of Zhou et al. [31], the pursuit strategy was designed by balancing the purposes of pursuing an evader and evading a defender through a comprehensive fuzzy evaluation. Wei et al. [32] proposed two layered guidance strategies based on the differential game theory to balance the purposes of evasion and pursuit. In the aforementioned literature, most cases in which the pursuer's strategy or evaluation function is known may not be accurate in practice. Nevertheless, to achieve its goal, the pursuer tries to change its strategy in the presence of a detected defender. Liang and Deng et al. [33] proposed a pursuer-role-switching strategy, where the pursuer adopts a roundabout evasion strategy when the defender threatens it and continues to pursue the evader when it is in a safe situation. Rubinsky and Gutman [34,35] derived a guidance law of the pursuer using a linear dynamics model and a full three-dimensional vector dynamics model, respectively, and provided a simplified sufficient condition for the pursuer to avoid the defender while capturing the evader.

From the literature on guidance law designs for pursuers mentioned above, it is clear that pursuer strategies are becoming more complex. First, this is reflected in the pursuer's ability to detect the presence of a defender and react to its maneuvers. Second, it is evident in the pursuer's ability to dynamically choose its own strategy mode or adjust the weights of its own evaluation function with respect to each target according to different situations. Considering such smart pursuers, designing collaborative defense strategies to enhance the survival rate of evaders is an important motivation for this study. The main contributions of this study are as follows: (1) Depending on the pursuer's control objective in the orbit pursuit-evasion-defense (OPED) scenario, its behavioral modes are modeled according to differential game theory and divided into an attack mode against evader maneuvers and an avoidance mode against defender maneuvers. (2) In response to the different behavioral patterns of the pursuer, a two-way cooperative optimal guidance law for the evader and defender is derived based on optimal control theory, which reduces the miss distance and control effort of the defender through cooperation between the evader and defender. (3) A mode recognition algorithm with a joint interactive multiple model (IMM) and smooth variable structure filtering (SVSF) is proposed to recognize the pursuer's intention through historical observation information, thereby executing the collaborative strategy in the corresponding mode.

The remainder of this paper is organized as follows. Section 2 describes the dynamic model of the OPED. The OPED studied in this paper occurs in the vicinity of a circular orbit; therefors, C-W equations are used to describe the relative motions of the spacecraft. Section 3 models the behavioral pattern of the pursuer based on differential game theory in conjunction with the two control purposes of the pursuer. A detailed derivation of the two-way cooperative optimal guidance law for the evader and defender, is provided in Section4 based on the pursuer's behavioral patterns. Section 5 uses several SVSFs to match the modes of the pursuer and combines them with an interactive multiple model-matching (IMM) algorithm to identify the pursuer's behavior based on historical observations, which in turn guides the defensive coalition to adopt the corresponding cooperative strategies. Section 6 demonstrates the effectiveness of the proposed algorithm in terms of strategy identification, state estimation, and defense performance through simulations. Finally, a summary of the study is provided and future work is envisioned.

2. Dynamics of the Orbit-Pursuit-Evasion-Defense Game

In order to better analyze the relative state changes between spacecrafts, this paper selects a circular orbital virtual satellite near each spacecraft to establish a coordinate system. Taking the center of mass of the virtual satellite as the origin, the *x*-axis coincides with the position vector of the virtual satellite, the *z*-axis coincides with the orbital angular momentum vector of the virtual satellite, and the *y*-axis and the other two axes form the right-hand spiral coordinate system, as shown in Fig. 1. In the process of research, we assume that (1) The spacecraft moves as a point; (2) The virtual satellite does not maneuver; (3) Only consider two-body gravitational model. Taking the pursuer as an example, the motion equation are written:

$$\begin{cases} \ddot{\boldsymbol{r}}_o = -\dfrac{\mu}{\left\|\boldsymbol{r}_o\right\|^3}\boldsymbol{r}_o \\ \ddot{\boldsymbol{r}} = - - \dfrac{\mu}{\left\|\boldsymbol{r}\right\|^3}\boldsymbol{r} + \boldsymbol{u} \end{cases} \tag{1}$$

$\left\|\cdot\right\|$ represents the second-order norm of the vector, μ is the earth's gravity constant, and $\boldsymbol{u}$ is the acceleration generated by the pursuer's engine. Define the relative position of the pursuer and virtual satellite as $\delta\boldsymbol{r} = \boldsymbol{r} - \boldsymbol{r}_o$, and write the motion equation of the relative position under the orbital coordinate system as follows:

$$\begin{aligned} &\delta\boldsymbol{r}'' = -\dot{\boldsymbol{\omega}} \times \delta\boldsymbol{r} - \boldsymbol{\omega} \times (\boldsymbol{\omega} \times \delta\boldsymbol{r}) - 2\boldsymbol{\omega} \times \delta\dot{\boldsymbol{r}} - \mu\left(\frac{\boldsymbol{r}}{\left\|\boldsymbol{r}\right\|^3} - \frac{\boldsymbol{r}_o}{\left\|\boldsymbol{r}_o\right\|^3}\right) + \boldsymbol{u} \\ &\boldsymbol{\omega} = \begin{bmatrix} 0 & 1 & 0 \end{bmatrix}^{\mathrm{T}} \omega \\ &\dot{\boldsymbol{\omega}} = \begin{bmatrix} 0 & 1 & 0 \end{bmatrix}^{\mathrm{T}} \dot{\omega} \end{aligned} \tag{2}$$

where ω is the orbital angular rate of the virtual satellite. Since the virtual satellite is a circular orbit satellite, there is $\dot{\omega} = 0$. If the relative distance between the pursuer and virtual satellite is far less than the orbital radius of the pursuer, there is $\left\|\delta\boldsymbol{r}\right\| / \left\|\boldsymbol{r}\right\| \ll 1$, Eq. (2) that can be simplified to the famous C-W equation.

$$\begin{cases} \ddot{x}_i = 3\omega^2 x_i + 2\omega\dot{y}_i + u_{xi} \\ \ddot{y}_i = -2\omega\dot{x}_i + u_{yi} \qquad ,i = \mathrm{E,P,D} \\ \ddot{z}_i = -\omega^2 z_i + u_{zi} \end{cases} \tag{3}$$

where the subscript $i = \mathrm{E,P,D}$ denotes variables associated with the evader, pursuer, and defender, respectively. Writing the dynamic equations in the matrix form yields

$$\dot{\boldsymbol{X}}_i = \boldsymbol{A}\boldsymbol{X}_i + \boldsymbol{B}\boldsymbol{U}_i$$
$$\boldsymbol{A} = \begin{bmatrix} 0 & 0 & 0 & 1 & 0 & 0 \\ 0 & 0 & 0 & 0 & 1 & 0 \\ 0 & 0 & 0 & 0 & 0 & 1 \\ 3\omega^2 & 0 & 0 & 0 & 2\omega & 0 \\ 0 & 0 & 0 & -2\omega & 0 & 0 \\ 0 & 0 & -\omega^2 & 0 & 0 & 0 \end{bmatrix} \quad (4)$$
$$\boldsymbol{B} = \begin{bmatrix} 0 & 0 & 0 \\ 0 & 0 & 0 \\ 0 & 0 & 0 \\ 1 & 0 & 0 \\ 0 & 1 & 0 \\ 0 & 0 & 1 \end{bmatrix}$$

where $\boldsymbol{X}_i = [x_i, y_i, z_i, \dot{x}_i, \dot{y}_i, \dot{z}_i]^{\mathrm{T}}$ is the state variable of each spacecraft and $\boldsymbol{U}_i = [u_{xi}, u_{yi}, u_{zi}]^{\mathrm{T}}$ is the control variable of each spacecraft, the direction can be arbitrary and the amplitude satisfies $\|\boldsymbol{U}_i\|_2 \le \rho_i, \rho_i > 0$.

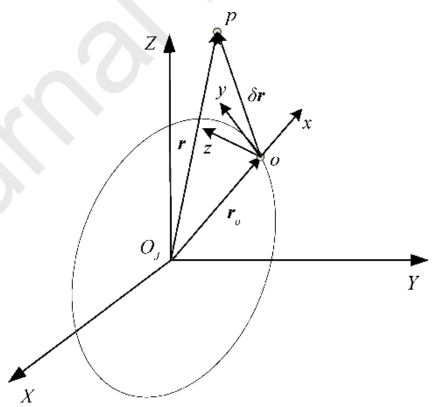

Fig. 1. Geocentric inertial coordinate system $O_J XYZ$ and orbital coordinate system $oxyz$.

Due to the relatively close distance between agents during the game, the devices on the pursuer, evader, and defender are able to detect each other's states. So the information set of the pursuer is $I_{\mathrm{P}}(t) = \left\{\boldsymbol{X}_{\mathrm{P}}(t), \boldsymbol{X}_{\mathrm{E}}(t), \boldsymbol{X}_{\mathrm{D}}(t)\right\}$. Compared with traditional pursuers, flexible pursuers are characterized by their ability to constantly change their own control objectives. Therefore, the strategy of pursuers is denoted as $\boldsymbol{U}_{\mathrm{P}}(I_{\mathrm{P}}(t), k_1, k_2)$, and k_1, k_2 is a parameter to measure the weights of the pursuers' control objectives, which will be introduced in the following section. Both the evader and defender can know the perfect state information of all agents, and estimate the strategy of the pursuer at the same time. The estimated strategy is denoted as $\tilde{\boldsymbol{U}}_{\mathrm{P}}$. The information set of the evader and defender is $I_{\mathrm{E}} = I_{\mathrm{D}} = \left\{ \boldsymbol{X}_{\mathrm{P}}(t), \boldsymbol{X}_{\mathrm{E}}(t), \boldsymbol{X}_{\mathrm{D}}(t), \tilde{\boldsymbol{U}}_{\mathrm{P}} \right\}$. From the perspective of the evader and defender, the goal is to find an optimal strategy that minimizes the following performance indicator.

$$
\begin{aligned}
J &= \frac{\alpha_{\mathrm{MD}}}{2} \boldsymbol{X}_{\mathrm{DP}}^{\mathrm{T}}(t_{f\mathrm{DP}}) \begin{bmatrix} \boldsymbol{I}_3 & \mathbf{0} \\ \mathbf{0} & \mathbf{0} \end{bmatrix} \boldsymbol{X}_{\mathrm{DP}}(t_{f\mathrm{DP}}) + \frac{\beta_{\mathrm{D}}}{2} \int_0^{t_{f\mathrm{DP}}} \boldsymbol{U}_{\mathrm{D}}^{\mathrm{T}} \boldsymbol{U}_{\mathrm{D}} \mathrm{d}t \\
&\quad + \frac{\beta_{\mathrm{E}}}{2} \int_0^{t_{f\mathrm{DP}}} \boldsymbol{U}_{\mathrm{E}}^{\mathrm{T}} \boldsymbol{U}_{\mathrm{E}} \mathrm{d}t \\
\boldsymbol{X}_{\mathrm{DP}} &= \boldsymbol{X}_{\mathrm{D}} - \boldsymbol{X}_{\mathrm{P}}
\end{aligned} \tag{5}
$$

$\alpha_{\mathrm{MD}}, \beta_{\mathrm{D}}, \beta_{\mathrm{E}}$ are positive constants, representing the weights of the defender's interception miss, defender's fuel consumption, and evader's fuel consumption. $t_{f\mathrm{DP}}$ represents the end time of the game between the pursuer and the defender. It can be seen from Eq. (5) that the calculation of performance indicators depends on the strategy of the pursuer, so how to estimate the strategy of the pursuer is the focus of this paper.

3. Pursuer strategy modeling

The pursuer has two goals throughout the game: circumventing the defender's interception and completing the evader's capture. In this section, the behavioral patterns of the pursuer will be modeled based on the differential game theory with respect to its two goals.

3.1. The game between the pursuer and evader

First, consider only the game between the evader and pursuer, and let the relative state be $\boldsymbol{X}_{\mathrm{PE}} = \boldsymbol{X}_{\mathrm{P}} - \boldsymbol{X}_{\mathrm{E}}$; the dynamical equations are as follows:

$$
\dot{\boldsymbol{X}}_{\mathrm{PE}} = \boldsymbol{A}\boldsymbol{X}_{\mathrm{PE}} + \boldsymbol{B}\boldsymbol{U}_{\mathrm{P}} - \boldsymbol{B}\boldsymbol{U}_{\mathrm{E}} \tag{6}
$$

Popular conventional guidance laws are proportional navigation (PN), augmented proportional navigation (APN), and optimal guidance law (OGL), where the differences exist mainly in the maneuvering assumptions of the evader and the consideration of different intelligent body autopilot dynamic models [36]. The PN guidance law assumes that the evader does not maneuver, APN assumes that the evader constantly maneuvers, and OGL considers a first-order autopilot dynamics model. In this study, we modeled the pursuer's strategy in a game with an evader based on the differential game theory. The evaluation function of the game between the pursuer and evader is defined as follows:

$$
\begin{aligned}
J_a &= \frac{1}{2} \boldsymbol{X}_{\mathrm{PE}}^{\mathrm{T}}(t_{f\mathrm{PE}}) \boldsymbol{Q} \boldsymbol{X}_{\mathrm{PE}}(t_{f\mathrm{PE}}) + \frac{\beta_{\mathrm{P}}}{2} \int_0^{t_{f\mathrm{PE}}} \boldsymbol{U}_{\mathrm{P}}^{\mathrm{T}} \boldsymbol{U}_{\mathrm{P}} \mathrm{d}t - \frac{\beta_{\mathrm{E}}}{2} \int_0^{t_{f\mathrm{PE}}} \boldsymbol{U}_{\mathrm{E}}^{\mathrm{T}} \boldsymbol{U}_{\mathrm{E}} \mathrm{d}t \\
\boldsymbol{Q} &= \begin{bmatrix} \bar{\alpha}_{\mathrm{MT}} \boldsymbol{I}_{3\times 3} & \mathbf{0}_{3\times 3} \\ \mathbf{0}_{3\times 3} & \mathbf{0}_{3\times 3} \end{bmatrix}
\end{aligned} \tag{7}
$$

where, $\bar{\alpha}_{\mathrm{MT}}, \beta_{\mathrm{P}}, \beta_{\mathrm{E}}$ are positive real numbers that represent the weights of different optimization objectives and $t_{f\mathrm{PE}}$ is the end moment of the game between the pursuer and evader. A zero-sum game is constituted between the pursuer and evader, and the pursuer requires Eq. (7) to be extremely small and the evader requires Eq.(7) to be extremely large.

For ease of presentation, the ZEM is defined as

$$\begin{aligned} &\boldsymbol{Z}_{\mathrm{PE}}(t)=\boldsymbol{D}\boldsymbol{\Phi}(t_{f\mathrm{PE}},t)\boldsymbol{X}_{\mathrm{PE}}(t) \\ &\boldsymbol{D}=\begin{bmatrix}\boldsymbol{I}_3 & \boldsymbol{0}_{3\times 3}\end{bmatrix}\end{aligned} \tag{8}$$

where, $\Phi(t_{f\mathrm{PE}},t)$ is the state transfer matrix that satisfies the following relationship:

$$\begin{aligned} &\dot{\boldsymbol{\Phi}}(t_{f\mathrm{PE}},t)=-\boldsymbol{\Phi}(t_{f\mathrm{PE}},t)\boldsymbol{A} \\ &\boldsymbol{\Phi}(t_{f\mathrm{PE}},t_{f\mathrm{PE}})=\boldsymbol{I}_6\end{aligned} \tag{9}$$

Solving Eq. (9) yields

$$\begin{aligned}
&\boldsymbol{\Phi}_{11}(t_{f\mathrm{PE}},t)=\begin{bmatrix} 4-3\cos(\omega\tau) & 0 & 0 \\ 6(\sin(\omega\tau)-\omega\tau) & 1 & 0 \\ 0 & 0 & \cos(\omega\tau)\end{bmatrix} \\
&\boldsymbol{\Phi}_{12}(t_{f\mathrm{PE}},t)=\begin{bmatrix} \dfrac{\sin(\omega\tau)}{\omega} & \dfrac{2(1-\cos(\omega\tau))}{\omega} & 0 \\ \dfrac{2(\cos(\omega\tau)-1)}{\omega} & \dfrac{4\sin(\omega\tau)-3\omega\tau}{\omega} & 0 \\ 0 & 0 & \dfrac{\sin(\omega\tau)}{\omega}\end{bmatrix} \\
&\boldsymbol{\Phi}_{21}(t_{f\mathrm{PE}},t)=\begin{bmatrix} 3\omega\sin(\omega\tau) & 0 & 0 \\ 6\omega(\cos(\omega)-1) & 0 & 0 \\ 0 & 0 & -\omega\sin(\omega\tau)\end{bmatrix} \\
&\boldsymbol{\Phi}_{22}(t_{f\mathrm{PE}},t)=\begin{bmatrix} \cos(\omega\tau) & 2\sin(\omega\tau) & 0 \\ -2\sin(\omega\tau) & 4\cos(\omega\tau)-3 & 0 \\ 0 & 0 & \cos(\omega\tau)\end{bmatrix}
\end{aligned} \tag{10}$$

where, $\tau=t_{f\mathrm{PE}}-t$. The physical meaning of ZEM is the relative position between the pursuer and evader when the system moves to the terminal moment from t, with $\boldsymbol{X}_{\mathrm{PE}}(t)$ as the initial state, and neither the pursuer nor the evader makes any maneuvers. The evaluation function can be rewritten according to the newly defined variables as follows:

$$J_a=\frac{\bar{\alpha}_{\mathrm{MT}}}{2}\boldsymbol{Z}_{\mathrm{PE}}^{\mathrm{T}}(t_{f\mathrm{PE}})\boldsymbol{Z}_{\mathrm{PE}}(t_{f\mathrm{PE}})+\frac{\beta_{\mathrm{P}}}{2}\int_0^{t_{f\mathrm{PE}}}\boldsymbol{U}_{\mathrm{P}}^{\mathrm{T}}\boldsymbol{U}_{\mathrm{P}}\mathrm{d}t-\frac{\beta_{\mathrm{E}}}{2}\int_0^{t_{f\mathrm{PE}}}\boldsymbol{U}_{\mathrm{E}}^{\mathrm{T}}\boldsymbol{U}_{\mathrm{E}}\mathrm{d}t \tag{11}$$

Deriving ZEM leads to a new equation of state:

$$\dot{\boldsymbol{Z}}_{\mathrm{PE}}(t)=\boldsymbol{D}\boldsymbol{\Phi}(t_{f\mathrm{PE}},t)(\boldsymbol{B}\boldsymbol{U}_{\mathrm{P}}(t)-\boldsymbol{B}\boldsymbol{U}_{\mathrm{E}}(t)) \tag{12}$$

Here, we directly write about saddle point strategy for the pursuer and evader.

$$\begin{aligned}\boldsymbol{U}_{\mathrm{P}}^{*}&=-\frac{\bar{\alpha}_{\mathrm{MT}}}{\beta_{\mathrm{P}}}\boldsymbol{\Phi}_{12}^{\mathrm{T}}(t_{f\mathrm{PE}},t)(\boldsymbol{I}_{3}+\frac{\bar{\alpha}_{\mathrm{MT}}}{\beta_{P}}\int_{t}^{t_{f\mathrm{PE}}}\boldsymbol{\Phi}_{12}\boldsymbol{\Phi}_{12}^{\mathrm{T}}\mathrm{d}\tau-\frac{\bar{\alpha}_{\mathrm{MT}}}{\beta_{\mathrm{E}}}\int_{t}^{t_{f\mathrm{PE}}}\boldsymbol{\Phi}_{12}\boldsymbol{\Phi}_{12}^{\mathrm{T}}\mathrm{d}\tau)^{-1}\boldsymbol{Z}_{\mathrm{PE}}(t)\\ \boldsymbol{U}_{\mathrm{E}}^{*}&=-\frac{\bar{\alpha}_{\mathrm{MT}}}{\beta_{\mathrm{E}}}\boldsymbol{\Phi}_{12}^{\mathrm{T}}(t_{f\mathrm{PE}},t)(\boldsymbol{I}_{3}+\frac{\bar{\alpha}_{\mathrm{MT}}}{\beta_{P}}\int_{t}^{t_{f\mathrm{PE}}}\boldsymbol{\Phi}_{12}\boldsymbol{\Phi}_{12}^{\mathrm{T}}\mathrm{d}\tau-\frac{\bar{\alpha}_{\mathrm{MT}}}{\beta_{\mathrm{E}}}\int_{t}^{t_{f\mathrm{PE}}}\boldsymbol{\Phi}_{12}\boldsymbol{\Phi}_{12}^{\mathrm{T}}\mathrm{d}\tau)^{-1}\boldsymbol{Z}_{\mathrm{PE}}(t)\end{aligned} \tag{13}$$

Saddle point solutions exist when $\beta_{\mathrm{E}} > \beta_{\mathrm{P}}$. For the convenience of the following discussion, substituting Eq. (10) into Eq. (13) and assuming $(\omega \to 0)$ yields:

$$\boldsymbol{U}_{\mathrm{P}}^{*}=-\frac{3\bar{\alpha}_{\mathrm{MT}}\beta_{E}}{3\beta_{\mathrm{P}}\beta_{\mathrm{E}}+(\beta_{\mathrm{E}}-\beta_{\mathrm{P}})\bar{\alpha}_{\mathrm{MT}}t_{\mathrm{goMT}}^{3}}t_{\mathrm{goMT}}\boldsymbol{Z}_{\mathrm{PE}}(t) \tag{14}$$

where, $t_{\mathrm{goMT}} = t_{f\mathrm{PE}} - t$. Notice that $\omega \to 0$ is a milder assumption when the orbital game occurs at high orbits. Assuming the pursuer needs to complete a precision hit on the evader, than $\bar{\alpha}_{\mathrm{MT}} \to \infty$ be obtained:

$$\boldsymbol{U}_{\mathrm{P}}^{*}=-\frac{3}{(1-\gamma_{1})t_{\mathrm{goMT}}^{2}}\boldsymbol{Z}_{\mathrm{PE}}(t) \tag{15}$$

where, $\gamma_{1}=\dfrac{\beta_{\mathrm{P}}}{\beta_{\mathrm{E}}}<1$. Eq. (15) represents a plausible strategy for the pursuer when the pursuer is not informed of the evader's specific strategy.

3.2. The Game Between the Defender and Pursuer

As discussed before, pursuer strategies are becoming increasingly complex, as evidenced by the pursuer's ability to perceive the presence of the defender and react to its maneuvers. This makes it necessary to model the game between the pursuer and defender, which significantly differs from the strategies adopted by the pursuer in the pursuit-evasion-defense game and traditional strategies such as PN and APN.

Similar to the previous section, we model the game between the pursuer and defender based on differential game theory. The evaluation function is defined as follows:

$$J_{d}=\frac{\bar{\alpha}_{\mathrm{MD}}}{2}\boldsymbol{Z}_{\mathrm{DP}}^{\mathrm{T}}(t_{f\mathrm{DP}})\boldsymbol{Z}_{\mathrm{DP}}(t_{f\mathrm{DP}})+\frac{\beta_{\mathrm{D}}}{2}\int_{0}^{t_{f\mathrm{DP}}}\boldsymbol{U}_{\mathrm{D}}^{\mathrm{T}}\boldsymbol{U}_{\mathrm{D}}\mathrm{d}t-\frac{\beta_{\mathrm{P}}}{2}\int_{0}^{t_{f\mathrm{DP}}}\boldsymbol{U}_{\mathrm{P}}^{\mathrm{T}}\boldsymbol{U}_{\mathrm{P}}\mathrm{d}t \tag{16}$$

where, $\bar{\alpha}_{\mathrm{MD}}, \beta_{\mathrm{D}}, \beta_{\mathrm{P}}$ are positive real numbers that represent the weights of the different objectives in the evaluation function and $\beta_{\mathrm{P}} > \beta_{\mathrm{D}}$. $\boldsymbol{Z}_{\mathrm{DP}}$ is the ZEM between the pursuer and defender, as defined in the previous section, and $t_{f\mathrm{DP}}$ is the end moment of the game between the pursuer and defender. The pursuer plays a game against the defender where the two sides constitute a zero-sum game, and the pursuer requires Eq. (16) to be extremely small and the defender requires Eq. (16) to be extremely large. We directly write the saddle point strategy for the game between the pursuer and defender as

$$\boldsymbol{U}_{\mathrm{P}}^{*}=-\frac{3\bar{\alpha}_{\mathrm{MD}}\beta_{\mathrm{D}}}{3\beta_{\mathrm{P}}\beta_{\mathrm{D}}+(\beta_{\mathrm{P}}-\beta_{\mathrm{D}})\bar{\alpha}_{\mathrm{MD}}t_{\mathrm{goMD}}^{3}}t_{\mathrm{goMD}}\boldsymbol{Z}_{\mathrm{DP}}(t) \tag{17}$$

where, $t_{\text{goMD}} = t_{f\text{DP}} - t$. Let $\bar{\alpha}_{\text{MD}} \to \infty$ to get:

$$\boldsymbol{U}_{\text{P}}^{*} = -\frac{3}{(\gamma_2 - 1)t_{\text{goMD}}^2}\boldsymbol{Z}_{\text{DP}}(t) \tag{18}$$

where, $\gamma_2 = \frac{\beta_{\text{P}}}{\beta_{\text{D}}} > 1$. When the pursuer has no further access to the defender's strategy, Eq. (18) is a reasonable strategy to ensure that the pursuer's gain is not less than the value of the zero-sum game.

When the pursuer plays only with the evader, its strategy is Eq. (15), and when the pursuer plays only with the defender, its strategy is Eq. (18). The following is a heuristic way to formulate the pursuer's strategy.

$$\boldsymbol{U}_{\text{P}} = -\frac{3k_1}{(1-\gamma_1)t_{\text{goMT}}^2}\boldsymbol{Z}_{\text{PE}}(t) - \frac{3k_2}{(\gamma_2 - 1)t_{\text{goMD}}^2}\boldsymbol{Z}_{\text{DP}}(t) \tag{19}$$

where, k_1, k_2 represent the weights of the two tasks of pursuing evaders and evading defenders in the pursuit task, respectively, and satisfy the following relationship:

$$0 \le k_1, k_2 \le 1, k_1 + k_2 = 1 \tag{20}$$

When $k_1 = 1, k_2 = 0$ the pursuer completely ignores the defender and plays only with the evader; when $k_1 = 0, k_2 = 1$ the pursuer completely ignores the evader and plays only with the defender. Fig. 2 shows the effect of different values of k_1, k_2 on the pursuer's trajectory. From the figure, it can be seen that although Eq. (19) is heuristically synthesized to obtain the pursuer strategy, the behavioral pattern of the pursuer during the pursuit-evasion-defense game can indeed be simulated by adjusting the value of k_1, k_2 during the game. For the definition of $t_{f\text{PE}}, t_{f\text{DP}}$ refer to the Ref. [37].

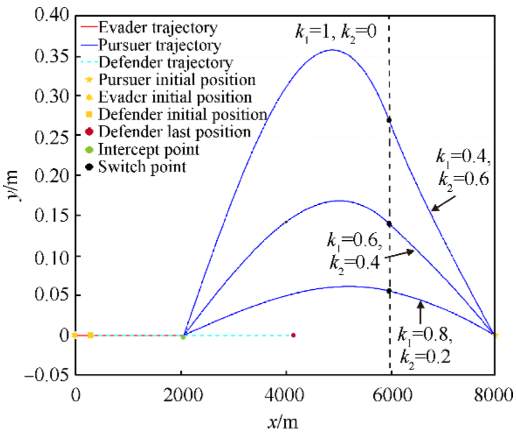

Fig. 2. The behavior of the pursuer is simulated by different values of k_1, k_2 in the vicinity of the collision trajectory.

4. Design of cooperative guidance

In a spacecraft active defense scenario, the control objective of the defending coalition is to intercept the pursuer before it captures the evader; therefore, the defender should minimize the miss distance between the pursuer. The evader should assist the defender in intercepting the pursuer with its own maneuvers because the pursuer is targeting it for guidance. The design of the cooperative guidance law is centered on controlling the defense team. We define the state of the game as $\boldsymbol{X}=\begin{bmatrix}\boldsymbol{X}_{\mathrm{P}}^{\mathrm{T}} & \boldsymbol{X}_{\mathrm{E}}^{\mathrm{T}} & \boldsymbol{X}_{\mathrm{D}}^{\mathrm{T}}\end{bmatrix}^{\mathrm{T}}$ and write the dynamic equations as follows:

$$\begin{gathered}\dot{\boldsymbol{X}}=\bar{\boldsymbol{A}}\boldsymbol{X}+\boldsymbol{B}_{\mathrm{P}}\boldsymbol{U}_{\mathrm{P}}+\boldsymbol{B}_{\mathrm{E}}\boldsymbol{U}_{\mathrm{E}}+\boldsymbol{B}_{\mathrm{D}}\boldsymbol{U}_{\mathrm{D}}\\ \bar{\boldsymbol{A}}=\begin{bmatrix}\boldsymbol{A} & \mathbf{0}_{6\times6} & \mathbf{0}_{6\times6}\\ \mathbf{0}_{6\times6} & \boldsymbol{A} & \mathbf{0}_{6\times6}\\ \mathbf{0}_{6\times6} & \mathbf{0}_{6\times6} & \boldsymbol{A}\end{bmatrix},\boldsymbol{B}_{\mathrm{P}}=\begin{bmatrix}\boldsymbol{B}\\ \mathbf{0}_{6\times3}\\ \mathbf{0}_{6\times3}\end{bmatrix}\\ \boldsymbol{B}_{\mathrm{E}}=\begin{bmatrix}\mathbf{0}_{6\times3}\\ \boldsymbol{B}\\ \mathbf{0}_{6\times3}\end{bmatrix},\boldsymbol{B}_{\mathrm{D}}=\begin{bmatrix}\mathbf{0}_{6\times3}\\ \mathbf{0}_{6\times3}\\ \boldsymbol{B}\end{bmatrix}\end{gathered}\tag{21}$$

Substituting the pursuer's strategy from the previous section into the dynamic equation.

$$\dot{\boldsymbol{X}}=\tilde{\boldsymbol{A}}(t)\boldsymbol{X}+\boldsymbol{B}_{\mathrm{E}}\boldsymbol{U}_{\mathrm{E}}+\boldsymbol{B}_{\mathrm{D}}\boldsymbol{U}_{\mathrm{D}}\tag{22}$$

where $\tilde{\boldsymbol{A}}=\begin{bmatrix}\tilde{\boldsymbol{A}}_{11}(t) & \tilde{\boldsymbol{A}}_{12}(t) & \tilde{\boldsymbol{A}}_{13}(t)\\ 0 & \boldsymbol{A} & 0\\ 0 & 0 & \boldsymbol{A}\end{bmatrix}$:

$$\begin{gathered}\tilde{\boldsymbol{A}}_{11}(t)=\boldsymbol{A}+\frac{3k_2}{(\gamma_2-1)t_{\mathrm{goMD}}^2}\boldsymbol{BD\Phi}(t_{f\mathrm{DP}},t)-\frac{3k_1}{(1-\gamma_1)t_{\mathrm{goMT}}^2}\boldsymbol{BD\Phi}(t_{f\mathrm{PE}},t)\\ \tilde{\boldsymbol{A}}_{12}(t)=\frac{3k_1}{(1-\gamma_1)t_{\mathrm{goMT}}^2}\boldsymbol{BD\Phi}(t_{f\mathrm{PE}},t)\\ \tilde{\boldsymbol{A}}_{13}(t)=-\frac{3k_2}{(\gamma_2-1)t_{\mathrm{goMD}}^2}\boldsymbol{BD\Phi}(t_{f\mathrm{DP}},t)\end{gathered}\tag{23}$$

The ZEM $\hat{\boldsymbol{Z}}_{\mathrm{DP}}(t)=\hat{\boldsymbol{D}}\hat{\boldsymbol{\Phi}}(t_{f\mathrm{DP}},t)\boldsymbol{X}(t)$, where $\hat{\boldsymbol{D}}=\boldsymbol{D}\begin{bmatrix}-\boldsymbol{I}_{6\times6} & \mathbf{0}_{6\times6} & \boldsymbol{I}_{6\times6}\end{bmatrix}$, $\hat{\boldsymbol{\Phi}}(t_{f\mathrm{DP}},t)$ is the state transfer matrix of Eq. (22), which satisfies

$$\begin{gathered}\dot{\hat{\boldsymbol{\Phi}}}(t_{f\mathrm{DP}},t)=-\hat{\boldsymbol{\Phi}}(t_{f\mathrm{DP}},t)\tilde{\boldsymbol{A}}(t)\\ \hat{\boldsymbol{\Phi}}(t_{f\mathrm{DP}},t_{f\mathrm{DP}})=\boldsymbol{I}_{18}\end{gathered}\tag{24}$$

The time derivatives of ZEM are

$$\begin{gathered}\dot{\hat{\boldsymbol{Z}}}_{\mathrm{DP}}(t)=\tilde{\boldsymbol{B}}_{\mathrm{E}}\boldsymbol{U}_{\mathrm{E}}+\tilde{\boldsymbol{B}}_{\mathrm{D}}\boldsymbol{U}_{\mathrm{D}}\\ \tilde{\boldsymbol{B}}_{\mathrm{E}}=\hat{\boldsymbol{D}}\hat{\boldsymbol{\Phi}}(t_{f\mathrm{DP}},t)\boldsymbol{B}_{\mathrm{E}},\tilde{\boldsymbol{B}}_{\mathrm{D}}=\hat{\boldsymbol{D}}\hat{\boldsymbol{\Phi}}(t_{f\mathrm{DP}},t)\boldsymbol{B}_{\mathrm{D}}\end{gathered}\tag{25}$$

Writing an evaluation function for the defense team using the newly defined ZEM:

$$J = \frac{\alpha_{MD}}{2} \boldsymbol{Z}_{DP}^{T}(t_{f\mathrm{DP}})\boldsymbol{Z}_{\mathrm{DP}}(t_{f\mathrm{DP}}) + \frac{\beta_{\mathrm{D}}}{2}\int_0^{t_{f\mathrm{DP}}} \boldsymbol{U}_{\mathrm{D}}^{\mathrm{T}}\boldsymbol{U}_{\mathrm{D}}\mathrm{d}t + \frac{\beta_{\mathrm{E}}}{2}\int_0^{t_{f\mathrm{DP}}} \boldsymbol{U}_{\mathrm{E}}^{\mathrm{T}}\boldsymbol{U}_{\mathrm{E}}\mathrm{d}t \tag{26}$$

where, $\alpha_{\mathrm{MD}}, \beta_{\mathrm{D}}, \beta_{\mathrm{E}}$ are positive real numbers, and the entire evaluation function consists of the miss distance of the defender at the terminal moment and the quadratic integral of the evader and defender controls. The optimal control strategy maintains a reasonable fuel consumption with the smallest possible defender miss distance. The Hamiltonian function is expressed as follows:

$$H = \frac{\beta_{\mathrm{D}}}{2}\boldsymbol{U}_{\mathrm{D}}^{\mathrm{T}}\boldsymbol{U}_{\mathrm{D}} + \frac{\beta_{\mathrm{E}}}{2}\boldsymbol{U}_{\mathrm{E}}^{\mathrm{T}}\boldsymbol{U}_{\mathrm{E}} + \boldsymbol{\lambda}^{\mathrm{T}}(\tilde{\boldsymbol{B}}_{\mathrm{E}}\boldsymbol{U}_{\mathrm{E}} + \tilde{\boldsymbol{B}}_{\mathrm{D}}\boldsymbol{U}_{\mathrm{D}}) \tag{27}$$

The optimal control of the evader and defender is derived from the following control equations:

$$\begin{aligned} &\frac{\partial H}{\partial \boldsymbol{U}_{\mathrm{D}}^{*}} = 0 \rightarrow \boldsymbol{U}_{\mathrm{D}}^{*} = -\frac{1}{\beta_{\mathrm{D}}}\tilde{\boldsymbol{B}}_{\mathrm{D}}^{\mathrm{T}}\boldsymbol{\lambda} \\ &\frac{\partial H}{\partial \boldsymbol{U}_{\mathrm{E}}^{*}} = 0 \rightarrow \boldsymbol{U}_{\mathrm{E}}^{*} = -\frac{1}{\beta_{\mathrm{E}}}\tilde{\boldsymbol{B}}_{\mathrm{E}}^{\mathrm{T}}\boldsymbol{\lambda} \end{aligned} \tag{28}$$

This can be obtained from the adjoint equations and the transversality condition:

$$\boldsymbol{\lambda} = \alpha_{\mathrm{MD}}\boldsymbol{Z}_{\mathrm{DP}}(t_{f\mathrm{DP}}) \tag{29}$$

Substituting Eq. (29) into the expression for optimal control:

$$\begin{aligned} \boldsymbol{U}_{\mathrm{D}}^{*} &= -\frac{\alpha_{\mathrm{MD}}}{\beta_{\mathrm{D}}}\tilde{\boldsymbol{B}}_{\mathrm{D}}^{\mathrm{T}}\boldsymbol{Z}_{\mathrm{DP}}(t_{f\mathrm{DP}}) \\ \boldsymbol{U}_{\mathrm{E}}^{*} &= -\frac{\alpha_{\mathrm{MD}}}{\beta_{\mathrm{E}}}\tilde{\boldsymbol{B}}_{\mathrm{E}}^{\mathrm{T}}\boldsymbol{Z}_{\mathrm{DP}}(t_{f\mathrm{DP}}) \end{aligned} \tag{30}$$

Substituting the optimal control into the rate of change of the ZEM and integrating from t to $t_{f\mathrm{DP}}$:

$$\begin{aligned} &\boldsymbol{Z}_{\mathrm{DP}}(t_{f\mathrm{DP}}) = \Xi\boldsymbol{Z}_{\mathrm{DP}}(t) \\ &\Xi = (\boldsymbol{I}_3 + \frac{\alpha_{\mathrm{MD}}}{\beta_{\mathrm{E}}}\int_t^{t_{f\mathrm{DP}}}\tilde{\boldsymbol{B}}_{\mathrm{E}}\tilde{\boldsymbol{B}}_{\mathrm{E}}^{\mathrm{T}}\mathrm{d}\tau + \frac{\alpha_{\mathrm{MD}}}{\beta_{\mathrm{D}}}\int_t^{t_{f\mathrm{DP}}}\tilde{\boldsymbol{B}}_{\mathrm{D}}\tilde{\boldsymbol{B}}_{\mathrm{D}}^{\mathrm{T}}\mathrm{d}\tau)^{-1} \end{aligned} \tag{31}$$

Substituting Eq. (31) into Eq. (30) yields the two-way cooperative optimal control of the evader and defender as follows:

$$\begin{aligned} \boldsymbol{U}_{D}^{*} &= -\frac{\alpha_{MD}}{\beta_{D}}\tilde{\boldsymbol{B}}_{D}^{T}\Xi\boldsymbol{Z}_{DP}(t) \\ \boldsymbol{U}_{E}^{*} &= -\frac{\alpha_{MD}}{\beta_{E}}\tilde{\boldsymbol{B}}_{E}^{T}\Xi\boldsymbol{Z}_{DP}(t) \end{aligned} \tag{32}$$

Throughout the computation of the cooperative strategy, it is necessary to know the task propensity of the pursuer, that is, k_1, k_2, which we discuss in the next section.

5. Pursuer pattern identification

In OPED, to achieve victory the pursuer has to flexibly shift between the attack and avoidance modes or flexibly change the evaluation weights between the two goals in its evaluation function to be able to take into account the two goals of pursuing the evader and evading the defender. Faced with an opponent having such a perception ability and intelligence level, if the defense team cannot obtain the pursuer's mode shift information and adopt a response strategy under the corresponding mode, it will reduce the efficiency of collaborative defense. In actual OPED, it is usually difficult for the defending team to have direct access to the pursuer's game intention; that is, it is difficult to determine the evaluation function of the pursuer at this point in time, which in turn makes it difficult to predict the pursuer's further actions. To address this problem, we identify pursuit strategies by designing an IMM algorithm. The algorithm comprises several parallel estimators, each of which corresponds to one of the pursuer's modes and updates the mode probability based on the likelihood function through Bayesian inference after each received measurement.

5.1. SVSF

The design basis of the SVSF algorithm is derived from the stability theory [38] and the inherent translation action ensures that the estimates converge close to the true value.The algorithm is a predictor-corrector estimator based on a sliding mode concept. The advantage of SVSF over other filtering algorithms is that it is highly stable with respect to uncertainty and noise in the given upper boundary. The more explicit the upper boundary, the better the performance of the SVSF. Unlike other filtering algorithms that only consider the estimation bias in the performance evaluation, SVSF has quantitative uncertainty and model bias evaluation indices for each estimated state or parameter, which can recover the estimation performance when there is a switch in the system mode and a sudden change in the system dynamics.

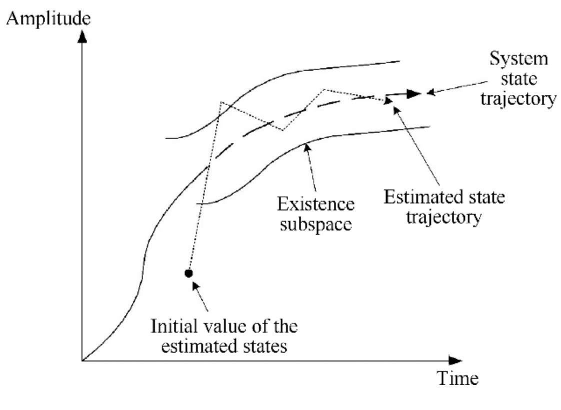

Fig. 3 Conceptual diagram of smooth variable structure filtering.

The basic estimation concept of the SVSF is illustrated in Fig. 3. The initial estimate is determined based on the designer's prior knowledge, and the region near the true-state trajectory is referred to as the existence subspace. Because of the effect of the SVSF gain, once the estimated state enters the existence subspace, it is confined to this region and follows a true-state trajectory. The width of the existential subspace is determined by the upper boundary of uncertainty and noise. The estimation error becomes larger if the width of the boundary layer is larger and if it is smaller oscillations arise in the estimated state. The derivation of the optimal boundary layer is given in the work [39]. The updated formula for the optimal boundary layer SVSF with the same observations and state dimensions is as follows:

$$\begin{aligned}
&\hat{\boldsymbol{X}}_{k/k-1} = \boldsymbol{\Phi}(k,k-1)\hat{\boldsymbol{X}}_{k-1/k-1} + \boldsymbol{B}_T\boldsymbol{U}_{k-1} \\
&\boldsymbol{P}_{k/k-1} = \boldsymbol{\Phi}(k,k-1)\boldsymbol{P}_{k-1/k-1}\boldsymbol{\Phi}^T(k,k-1) + \boldsymbol{Q}_{k-1} \\
&\boldsymbol{e}_{k/k-1} = \boldsymbol{z}_k - \boldsymbol{H}_k\hat{\boldsymbol{X}}_{k/k-1} \\
&\boldsymbol{\Psi}_k = \left(\boldsymbol{H}_k\boldsymbol{P}_{k/k-1}\boldsymbol{H}_k^T + \boldsymbol{R}_k\right)(\boldsymbol{P}_{k/k-1})^{-1}\left(\left|\boldsymbol{e}_{k/k-1}\right| + \gamma\left|\boldsymbol{e}_{k-1/k-1}\right|\right) \\
&\boldsymbol{K}_k = \mathrm{diag}[(\left|\boldsymbol{e}_{k/k-1}\right| + \gamma\left|\boldsymbol{e}_{k-1/k-1}\right|)\circ \mathrm{sat}(\boldsymbol{e}_{k/k-1},\boldsymbol{\Psi}_k)]\mathrm{diag}^{-1}(\boldsymbol{e}_{k/k-1}) \\
&\hat{\boldsymbol{X}}_{k/k} = \hat{\boldsymbol{X}}_{k/k-1} + \boldsymbol{K}_k\boldsymbol{e}_{k/k-1} \\
&\boldsymbol{P}_{k/k} = (\boldsymbol{I} - \boldsymbol{K}_k\boldsymbol{H}_k)\boldsymbol{P}_{k/k-1}(\boldsymbol{I} - \boldsymbol{K}_k\boldsymbol{H}_k)^{\mathrm{T}} + \boldsymbol{K}_k\boldsymbol{R}_k\boldsymbol{K}_k^{\mathrm{T}} \\
&\boldsymbol{e}_{k/k} = \boldsymbol{z}_k - \boldsymbol{H}_k\hat{\boldsymbol{X}}_{k/k}
\end{aligned} \tag{33}$$

where, $\circ$ represents the Schur product and $\mathrm{sat}(\boldsymbol{a},\boldsymbol{b})$ is the saturation function, which is defined as follows:

$$\mathrm{sat}_i(\boldsymbol{a},\boldsymbol{b}) = \begin{cases} a_i/b_i, \left|a_i/b_i\right| \le 1 \\ \mathrm{sgn}(a_i/b_i), \left|a_i/b_i\right| > 1 \end{cases} \tag{34}$$

$\boldsymbol{\Psi}_k, \boldsymbol{K}_k$ represent the width of the smoothing boundary layer and filter correction term, respectively. $\boldsymbol{Q}_{k-1}, \boldsymbol{R}_k$ are the process noise and measurement noise covariance matrices, respectively. $\boldsymbol{z}_k$ denotes the noise measurement at moment k.

5.2. Interacting Multiple Model (IMM) Algorithm

In the IMM algorithm, each filter matches a mode and operates in parallel to make state predictions based on the dynamics modeled in that mode. The IMM algorithm ultimately outputs a probability distribution over a set of modes, and the final state estimate is a mixture of different filters a posteriori estimates under that probability distribution. It also outputs the probabilities of different modes, and a mode that is closer to the real situation will have a greater probability. The IMM algorithm updates the pattern probability distribution at each step through Bayesian inference using historical observations. The probability corresponding to a mode that is close to the real situation gradually converges to a larger value.

In this study, the pursuer's strategy is discretized into four modes, $(k_1,k_2)\in\{(0.8,0.2),(0.6,0.4),(0.4,0.6),(0.2,0.8)\}$. The larger the value of k_1 the more the pursuer tends to play with the evader, and the larger the value of k_2 the more the pursuer tends to play with the defender. The pursuer's strategy is defined as the four corresponding modes based on the discretized k_1, k_2:

$$\boldsymbol{U}_{\mathrm{P}j} \in \{\boldsymbol{U}_{\mathrm{P1}},\boldsymbol{U}_{\mathrm{P2}},\boldsymbol{U}_{\mathrm{P3}},\boldsymbol{U}_{\mathrm{P4}}\},\ j=1,2,3,4$$
$$\boldsymbol{U}_{\mathrm{P}j} = -\frac{3k_{1j}}{(1-\gamma_1)t_{\mathrm{goMT}}^{2}}\boldsymbol{Z}_{\mathrm{PE}}(t) - \frac{3k_{2j}}{(\gamma_2-1)t_{\mathrm{goMD}}^{2}}\boldsymbol{Z}_{\mathrm{DP}}(t) \tag{35}$$

In this study, it was assumed that the γ_1,γ_2 in Eq. (35) are $0,3$ respectively. If this assumption does not hold, the values of γ_1,γ_2 can also be set as the parameters to be recognized and added to the model.

The flowchart of the algorithm is shown in Fig. 4.

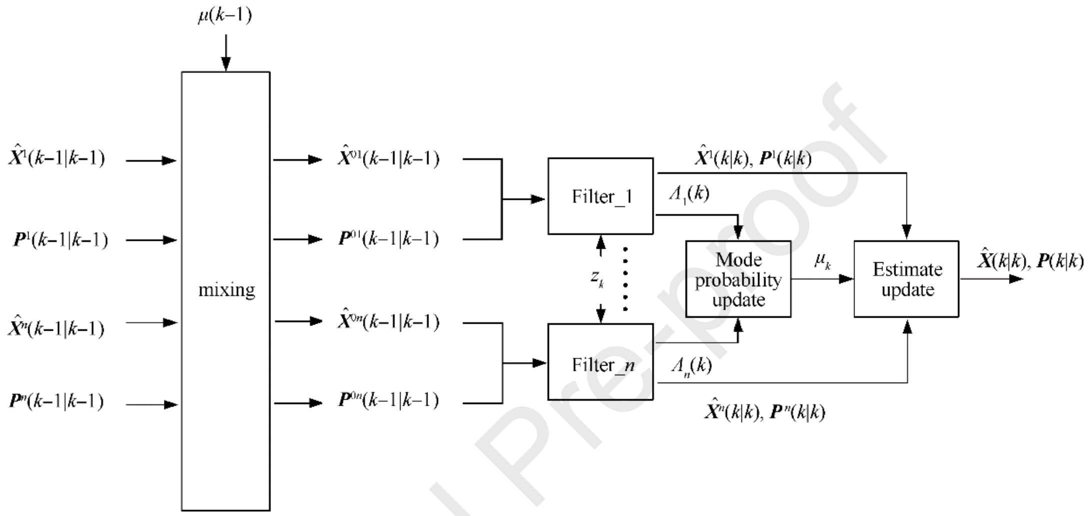

Fig. 4. Flowchart of the IMM algorithm.

The steps in each update cycle are as follows:

(1) Mixing

The Markov matrix that represents the transition probabilities between modes is first defined:

$$P_{ij} = \mathrm{Prob}\{\boldsymbol{U}_{\mathrm{P}/k} = \boldsymbol{U}_{\mathrm{P}j} \mid \boldsymbol{U}_{\mathrm{P}/k\text{-}1} = \boldsymbol{U}_{Pi}\}, i,\ j=1,2,3,4 \tag{36}$$

P_{ij} denotes the probability that the current moment is model j if the previous moment was model i. The Markov matrix belongs to the design parameters of the IMM algorithm and should be specified by the designer. According to the literature[40], the final results are not sensitive to this parameter.

The mode mixing probability is defined as follows:

$$\mu_{k-1/k-1}^{i|j} = \frac{1}{c_j} p_{ij}\mu_{k-1}^{i} \tag{37}$$

where, $c_j = \sum_{i=1}^{4} p_{ij}\mu_{k-1}^{i}$ and μ_{k-1}^{i} represent the probability of mode i in the previous step. The initial value of each estimator is obtained by mixing the posteriori estimates of each estimator from the previous step.

$$
\begin{aligned}
&\hat{\boldsymbol{X}}_{k-1/k-1}^{0j}=\sum_{i=1}^{4}[\hat{\boldsymbol{X}}_{k-1/k-1}^{i}\mu_{k-1/k-1}^{i|j}] \\
&\boldsymbol{P}_{k-1/k-1}^{0j}=\sum_{i=1}^{4}\{[\boldsymbol{P}_{k-1/k-1}^{i}+(\hat{\boldsymbol{X}}_{k-1/k-1}^{i}-\hat{\boldsymbol{X}}_{k-1/k-1}^{0j})(\hat{\boldsymbol{X}}_{k-1/k-1}^{i}-\hat{\boldsymbol{X}}_{k-1/k-1}^{0j})^{T}]\mu_{k-1/k-1}^{i|j}\}
\end{aligned}
\tag{38}
$$

(2) Mode matching

Writing the dynamic equations of the system.

$$
\dot{\boldsymbol{X}}=\begin{bmatrix}\boldsymbol{A}&0&0\\0&\boldsymbol{A}&0\\0&0&\boldsymbol{A}\end{bmatrix}\boldsymbol{X}+\begin{bmatrix}\boldsymbol{B}&0&0\\0&\boldsymbol{B}&0\\0&0&\boldsymbol{B}\end{bmatrix}\begin{bmatrix}\boldsymbol{U}_{\mathrm{P}}\\\boldsymbol{U}_{\mathrm{E}}\\\boldsymbol{U}_{\mathrm{D}}\end{bmatrix}
\tag{39}
$$

The pursuer's strategy is

$$
\boldsymbol{U}_{\mathrm{P}j}=-\frac{3k_{1j}}{(1-\gamma_1)t_{\mathrm{goMT}}^2}\boldsymbol{Z}_{\mathrm{PE}}(t)-\frac{3k_{2j}}{(\gamma_2-1)t_{\mathrm{goMD}}^2}\boldsymbol{Z}_{\mathrm{DP}}(t)
\tag{40}
$$

Substituting this into Eq. (39) and writing it in the matrix form yields

$$
\begin{aligned}
&\dot{\boldsymbol{X}}=\hat{\boldsymbol{A}}_j\boldsymbol{X}+\hat{\boldsymbol{B}}\boldsymbol{U} \\
&\tilde{\boldsymbol{A}}_j=\begin{bmatrix}\tilde{\boldsymbol{A}}_{11}^{j}(t)&\tilde{\boldsymbol{A}}_{12}^{j}(t)&\tilde{\boldsymbol{A}}_{13}^{j}(t)\\0&\boldsymbol{A}&0\\0&0&\boldsymbol{A}\end{bmatrix} \\
&\tilde{\boldsymbol{A}}_{11}^{j}(t)=\boldsymbol{A}+\frac{3k_{2j}}{(\gamma_2-1)t_{\mathrm{goMD}}^2}\boldsymbol{BD\Phi}(t_{f\mathrm{DP}},t)-\frac{3k_{1j}}{(1-\gamma_1)t_{\mathrm{goMT}}^2}\boldsymbol{BD\Phi}(t_{f\mathrm{PE}},t) \\
&\tilde{\boldsymbol{A}}_{12}^{j}(t)=\frac{3k_{1j}}{(1-\gamma_1)t_{\mathrm{goMT}}^2}\boldsymbol{BD\Phi}(t_{f\mathrm{PE}},t) \\
&\tilde{\boldsymbol{A}}_{13}^{j}(t)=-\frac{3k_{2j}}{(\gamma_2-1)t_{\mathrm{goMD}}^2}\boldsymbol{BD\Phi}(t_{f\mathrm{DP}},t) \\
&\hat{\boldsymbol{B}}=\begin{bmatrix}\boldsymbol{0}_{9\times6}\\ [\boldsymbol{I}_{3\times3},\boldsymbol{0}_{3\times3}]\\ \boldsymbol{0}_{3\times6}\\ [\boldsymbol{0}_{3\times3},\boldsymbol{I}_{3\times3}]\end{bmatrix}
\end{aligned}
\tag{41}
$$

where, $\boldsymbol{U}=[\boldsymbol{U}_{\mathrm{E}}^{\mathrm{T}},\boldsymbol{U}_{\mathrm{D}}^{\mathrm{T}}]^{\mathrm{T}}$. Writing Eq. (41) in discretized form gives

$$
\boldsymbol{X}_k=\hat{\boldsymbol{\Phi}}_j(k,k-1)\boldsymbol{X}_{k-1}+\boldsymbol{B}_T\boldsymbol{U}+\boldsymbol{W}_{k-1}
\tag{42}
$$

where, $\hat{\boldsymbol{\Phi}}_j(k,k-1)$ is the state transfer matrix of the system in Eq. (41), calculated according to the following equation:

$$
\hat{\boldsymbol{\Phi}}_j(k,k-1)=e^{\hat{A}_jT}
\tag{43}
$$

where, T is the step size of the one-step state prediction. Notice that Eq. (43) is reasonable when T

is sufficiently small, even though the coefficient matrix of Eq. (41) is time-varying. The observation equations of the system are the same for all the modes.

$$\boldsymbol{z}_k = \boldsymbol{H}_k \boldsymbol{X}_k + \boldsymbol{V}_k \tag{44}$$

$\boldsymbol{W}, \boldsymbol{V}$ represent the process and measurement noise, both of which are Gaussian white noise, and the covariance matrices are $\boldsymbol{Q}, \boldsymbol{R}$. The filters matched to each mode perform state estimation in parallel based on the state transfer matrix $\hat{\boldsymbol{\Phi}}_j(k, k-1)$ and output their respective state estimates and state covariance matrices.

$$\begin{aligned}
&\hat{\boldsymbol{X}}^j_{k/k-1} = \hat{\boldsymbol{\Phi}}_j(k,k-1)\hat{\boldsymbol{X}}^j_{k-1/k-1} + \boldsymbol{B}_T\boldsymbol{U}_{k-1}\\
&\boldsymbol{P}^j_{k/k-1} = \hat{\boldsymbol{\Phi}}_j(k,k-1)\boldsymbol{P}^j_{k-1/k-1}\hat{\boldsymbol{\Phi}}_i^{\mathrm{T}}(k,k-1) + \boldsymbol{Q}_{k-1}\\
&\boldsymbol{e}^j_{k/k-1} = \boldsymbol{z}_k - \boldsymbol{H}_k\hat{\boldsymbol{X}}^j_{k/k-1}\\
&\boldsymbol{\Psi}^j_k = (\boldsymbol{H}_k\boldsymbol{P}^j_{k/k-1}\boldsymbol{H}_k^T + R_k)(\boldsymbol{P}^j_{k/k-1})^{-1}(\left|\boldsymbol{e}^j_{k/k-1}\right| + \gamma\left|\boldsymbol{e}^j_{k-1/k-1}\right|)\\
&\boldsymbol{K}^j_k = diag[(\left|\boldsymbol{e}^j_{k/k-1}\right| + \gamma\left|\boldsymbol{e}^j_{k-1/k-1}\right|)\circ \mathrm{sat}(\boldsymbol{e}^j_{k/k-1}, \boldsymbol{\Psi}^j_k)]\mathrm{diag}^{-1}(\boldsymbol{e}^j_{k/k-1})\\
&\hat{\boldsymbol{X}}^j_{k/k} = \hat{\boldsymbol{X}}^j_{k/k-1} + \boldsymbol{K}^j_k\boldsymbol{e}^j_{k/k-1}\\
&\boldsymbol{P}^j_{k/k} = (\boldsymbol{I} - \boldsymbol{K}^j_k\boldsymbol{H}_k)\boldsymbol{P}^j_{k/k-1}(\boldsymbol{I} - \boldsymbol{K}^j_k\boldsymbol{H}_k)^T + \boldsymbol{K}^j_k\boldsymbol{R}_K\boldsymbol{K}^{jT}_k
\end{aligned} \tag{45}$$

(3) Mode probability updates

The initial value of the mode probability is defined as μ^j_0 and is determined empirically. The probability that the mode of step k is j can be written in the form of a Bayesian inference as:

$$\mu^j_k = \mathrm{Prob}\{\boldsymbol{U}_{\mathrm{P}j} \mid \boldsymbol{z}_{1:k}\} = \frac{p(\boldsymbol{z}_k \mid \boldsymbol{z}_{1:k-1}, \boldsymbol{U}_{Pj})}{p(\boldsymbol{z}_k \mid \boldsymbol{z}_{1:k-1})}\mu^j_{k-1} \tag{46}$$

where, $\boldsymbol{z}_{1:k} \triangleq \{\boldsymbol{z}_i, i = 1, 2, \cdots k\}$. According to the Ref. [40], the updated formula for the model probability is

$$\mu^j_k = \frac{\Lambda^j_k c_j}{c} \tag{47}$$

where, $\Lambda^j_k = \mathrm{prob}\{\boldsymbol{z}_k \mid \boldsymbol{z}_{1:k-1}, \boldsymbol{U}_{pj}\}$ is the likelihood function and $c = \sum_{j=1}^{4}\Lambda^j_k c_j$. The likelihood function is obtained using the following equation:

$$\Lambda^j_k = \mathcal{N}(\boldsymbol{v}^j_k; \boldsymbol{0}, \boldsymbol{S}^j_k) \tag{48}$$

where, $\boldsymbol{v}^j_k = \boldsymbol{z}_k - \boldsymbol{H}_k\hat{\boldsymbol{X}}^j_{k/k-1}$ is the innovation, $\boldsymbol{S}^j_k = \boldsymbol{P}^j_{k-1/k-1} + \boldsymbol{R}_k$ is the covariance matrix, and $\mathcal{N}(\boldsymbol{v}^j_k; \boldsymbol{0}, \boldsymbol{S}^j_k)$ is the probability density function of $\boldsymbol{v}^j_k$ when the mean is $\boldsymbol{0}$ and the covariance matrix is $\boldsymbol{S}^j_k$.

$$\mathcal{N}(\boldsymbol{v}^j_k; \boldsymbol{0}, \boldsymbol{S}^j_k) \triangleq |2\pi\boldsymbol{S}^j_k|^{-1/2}\,\mathrm{e}^{-\frac{1}{2}(\boldsymbol{v}^j_k)^{\mathrm{T}}(\boldsymbol{S}^j_k)^{-1}\boldsymbol{v}^j_k} \tag{49}$$

The final state estimate and the covariance of the entire filtering algorithm are

$$\hat{\boldsymbol{X}}_{k/k} = \sum_{j=1}^{4} \mu_k^j \hat{\boldsymbol{X}}_{k/k}^j$$
$$\boldsymbol{P}_{k/k} = \sum_{j=1}^{4} \mu_k^j [\boldsymbol{P}_{k/k}^j + (\hat{\boldsymbol{X}}_{k/k} - \hat{\boldsymbol{X}}_{k/k}^j)(\hat{\boldsymbol{X}}_{k/k} - \hat{\boldsymbol{X}}_{k/k}^j)^{\mathrm{T}}] \tag{50}$$

The mode assumed the pursuer is estimated according to the following rule. The mode corresponding to the maximum probability of the estimator output is the estimated mode.

$$\hat{\boldsymbol{U}}_{\mathrm{P}} = \hat{\boldsymbol{U}}_{\mathrm{P}j},\ j = \arg\max \mu_k^j \tag{51}$$

The evader and defender will take cooperative control in the corresponding mode.

6. Simulation analysis

In this section, numerical simulations will be used to demonstrate the effectiveness of the collaborative defense strategy based on the IMM mode recognition algorithm proposed in this study in active defense scenarios. The OPED considered in this section takes place in a synchronous orbit; therefore, a virtual synchronous orbit satellite in the vicinity of the three spacecraft involved in the game is selected to establish the coordinate system, and the orbital angular rate of this virtual satellite is $\omega = 7.27 \times 10^{-5}$ rad/s . First, let us consider two sample runs. In the first scenario, the pursuer first adopts the $k_1 = 0.8, k_2 = 0.2$ strategy, and after 5s it switches to the $k_1 = 0.4, k_2 = 0.6$ strategy. In the second sample run, the pursuer performs two strategy switches, in addition to the strategy switch in the first sample run, and after 10 s the pursuer switches again to the $k_1 = 0.6, k_2 = 0.4$. The initial positions of the pursuer, evader and defender are $[8000; -2000; 1000]$ m , $[0; 0; 0]$ m and $[300; -200; 0]$ m respectively, and the initial speeds are $[-200; 0; 0]$ m/s , $[150; 0; 0]$ m/s , and $[200; 0; 0]$ m/s , respectively. The process noise and measurement noise covariance matrices are

$$\boldsymbol{Q} = \begin{bmatrix} \boldsymbol{Q}_1 & \boldsymbol{0}_{6\times6} & \boldsymbol{0}_{6\times6} \\ \boldsymbol{0}_{6\times6} & \boldsymbol{Q}_1 & \boldsymbol{0}_{6\times6} \\ \boldsymbol{0}_{6\times6} & \boldsymbol{0}_{6\times6} & \boldsymbol{Q}_1 \end{bmatrix}$$
$$\boldsymbol{R} = \begin{bmatrix} \boldsymbol{R}_1 & \boldsymbol{0}_{6\times6} & \boldsymbol{0}_{6\times6} \\ \boldsymbol{0}_{6\times6} & \boldsymbol{R}_1 & \boldsymbol{0}_{6\times6} \\ \boldsymbol{0}_{6\times6} & \boldsymbol{0}_{6\times6} & \boldsymbol{R}_1 \end{bmatrix} \tag{52}$$
$$\boldsymbol{Q}_1 = \mathrm{diag}\{[6\times10^{-3}, 6\times10^{-3}, 6\times10^{-3}, 1\times10^{-3}, 1\times10^{-3}, 1\times10^{-3}]\}$$
$$\boldsymbol{R}_1 = \mathrm{diag}\{[10^{-3}, 10^{-3}, 10^{-3}, 10^{-4}, 10^{-4}, 10^{-4}]\}$$

The initial value of the state estimation covariance matrix is

$$\boldsymbol{P}_0 = \begin{bmatrix} \boldsymbol{P}_1 & \boldsymbol{0}_{6\times6} & \boldsymbol{0}_{6\times6} \\ \boldsymbol{0}_{6\times6} & \boldsymbol{P}_1 & \boldsymbol{0}_{6\times6} \\ \boldsymbol{0}_{6\times6} & \boldsymbol{0}_{6\times6} & \boldsymbol{P}_1 \end{bmatrix} \quad (53)$$

$$\boldsymbol{P}_1 = \mathrm{diag}\{[1,1,1,0.1,0.1,0.1]\}$$

The Markov matrix is

$$\begin{bmatrix} 0.94 & 0.02 & 0.02 & 0.02 \\ 0.02 & 0.94 & 0.02 & 0.02 \\ 0.02 & 0.02 & 0.94 & 0.02 \\ 0.02 & 0.02 & 0.02 & 0.94 \end{bmatrix} \quad (54)$$

First, we define the constant mode strategy (CM); that is, the defense team assumes that the pursuer always maintains the initial moment mode without switching throughout the game. Fig. 5 to **Error! Reference source not found.** show the simulation results for case 1. Fig. 5 shows a projection of the game trajectory onto the XOY plane. It can be observed that the trajectories of the IMM and CM strategies almost overlap before the strategy switch of the pursuer occurs, and the trajectories are shifted after the switch. The final miss distance of the defender under the IMM strategy is 0.4 m and under the CM strategy is 163 m. Fig. 6 shows the control amplitude curves of the defender, from which it can be observed that the two amplitude curves overlap before the pursuer's strategy switch, and the defender's control amplitude under the IMM strategy changes abruptly and is higher than that under the CM strategy in about 5 s owing to the pursuer's strategy switch. Subsequently, the control amplitude in the IMM strategy gradually decreases, whereas in the CM strategy it gradually increases. As can be seen from Fig. 7, the switch in the pursuer's strategy causes the defender's fuel consumption in the IMM strategy to exceed that of the CM strategy for a short period after the switch occurs. However, because the IMM strategy accurately recognizes the pursuer's mode, the fuel consumption gradually slows down, and ultimately consumes approximately half of that of the CM strategy. Fig. 8 shows the posterior probability plots for the various modes, from which it can be observed that the IMM algorithm quickly recognizes the mode used by the pursuer after the game starts and after the switch occurs. **Error! Reference source not found.** and **Error! Reference source not found.** show the estimation of the pursuer's position and velocity. It can be seen that the estimation of the pursuer's state converges very quickly after the realization of the pursuer's mode recognition.

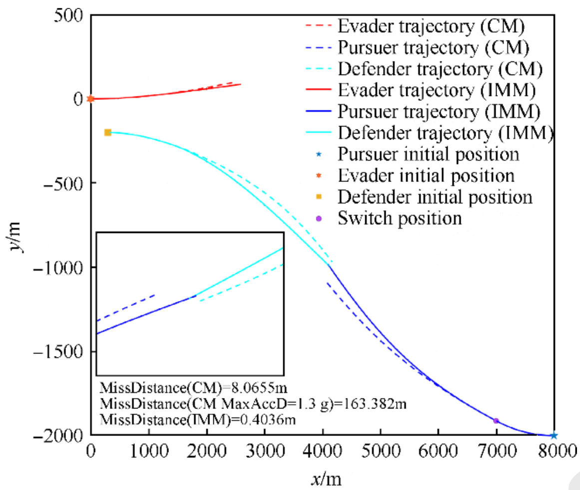

Fig. 5. *XOY* planar trajectories of the defensive team adopting CM and IMM strategies, respectively.

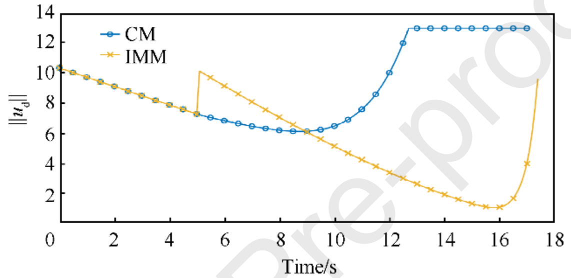

Fig. 6. Defender control amplitude curves under the IMM strategy and CM strategy.

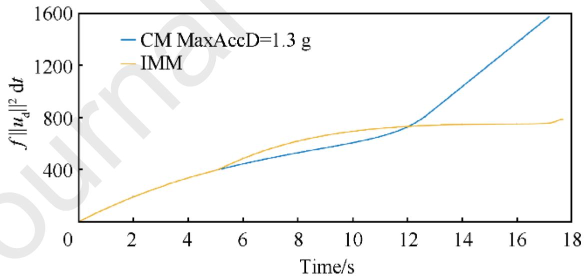

Fig. 7. Fuel consumption curves of the defender under the IMM strategy and CM strategy.

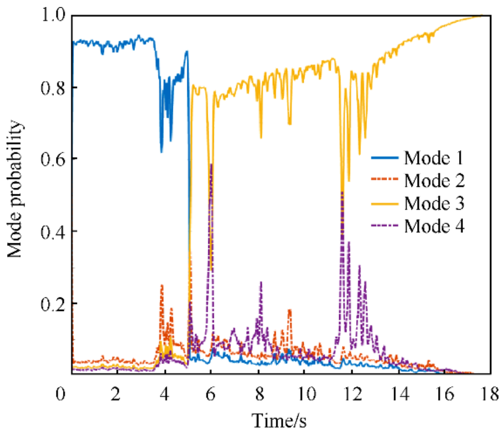

Fig. 8. Posterior probability curves for various modes of the pursuer.

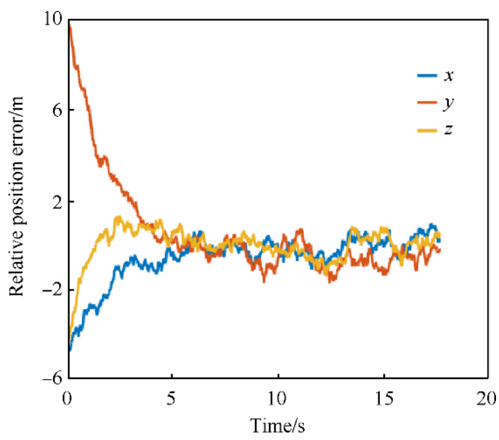

Fig 9. Error curves for pursuer position estimation.

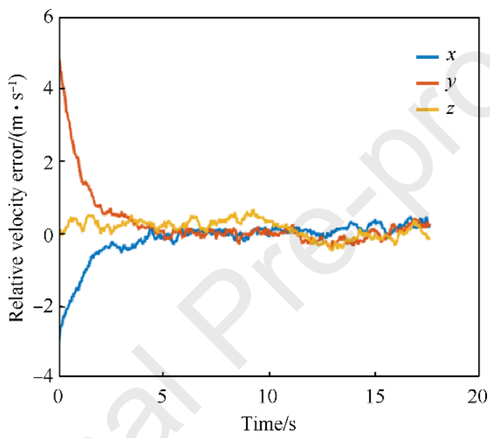

Fig. 10. Error curves for pursuer velocity estimation.

Error! Reference source not found. to **Error! Reference source not found.** show the simulation results for case 2. From **Error! Reference source not found.**, it is evident that the defender's miss distance was 25.1016 m for the CM strategy and 0.1728 m for the IMM strategy. **Error! Reference source not found.** reflects the trajectories corresponding to the values of different $\beta_{\mathrm{D}}, \beta_{\mathrm{E}}$ of the Eq. (26). It can be seen from the figure that the smaller the ratio of β_{D} to β_{E}, the more vigorous the maneuver of the defender, on the contrary, the more violent the evader maneuvered. In practical application, suitable parameters can be selected according to the mobility of the evader and defender. Fig. 9 and Fig. 10 show the control amplitude and fuel consumption curves of the defender, respectively.

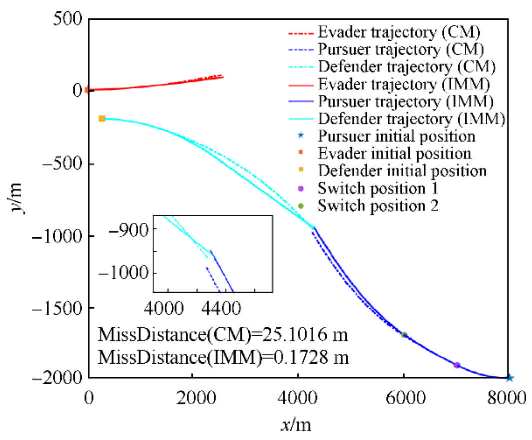

Fig. 11. *XOY* planar trajectories of the defensive team adopting CM and IMM strategies respectively.

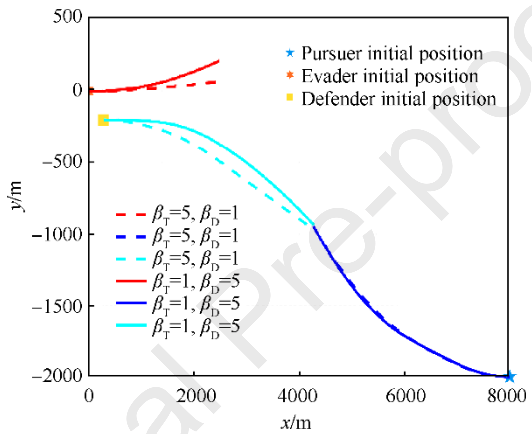

Fig. 12. Game trajectories under different parameters

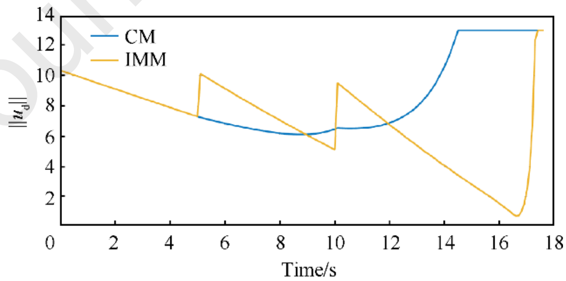

Fig. 9. Defender control amplitude curves under the IMM strategy and CM strategy.

It can be observed that when the pursuer's strategy is switched, the control amplitude of the defender under the IMM strategy undergoes an abrupt change owing to the IMM algorithm's recognition of the pursuer's strategy; however, overall the control amplitude required by the defender under the IMM strategy is smaller than that of the CM strategy, as there is no saturation phenomenon. The fuel consumption was also lower in the IMM strategy was lower the CM strategy throughout the game. Fig. 11 shows the posterior probability of each pursuer mode of the pursuer switches. The IMM algorithm accurately captured the current mode of the pursuer from the observed data. **Error! Reference source not found.** and **Error! Reference source not found.** show the pursuer position and velocity estimation errors, respectively.

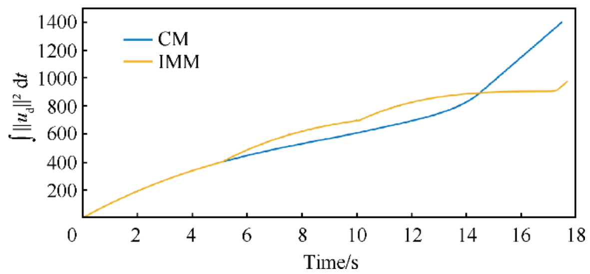

Fig. 10. Fuel consumption curves of the defender under the IMM strategy and CM strategy.

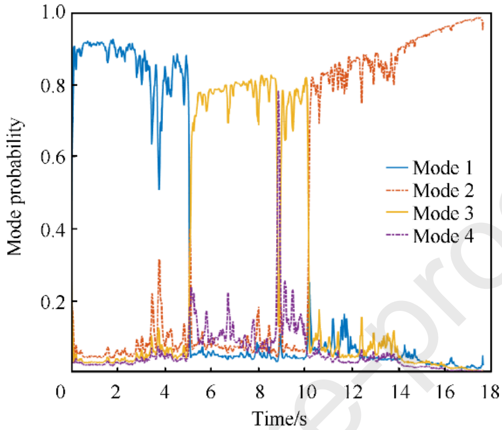

Fig. 11. Posterior probability curves for various modes of the pursuer.

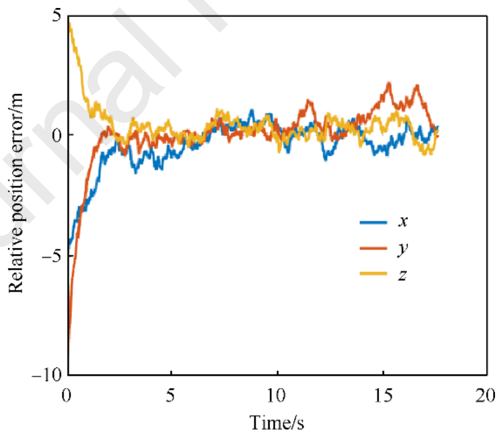

Fig. 16 Error curves to estimate pursuer position.

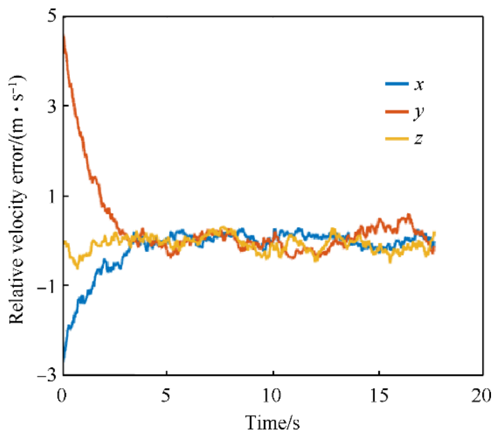

Fig. 17. Error curves to estimate pursuer velocity.

In the following, we analyze the effect of the pursuer's switching time on the outcome of the game. The strategy switching time of the pursuer was defined as t_{sw}. Other parameters are exactly the same as in case 1, and Fig. 12 shows the curve of the effect of switching time on the miss distance. As can be seen in Fig. 12, the miss distance is negatively correlated with t_{sw} under the CM strategy, which is expected. This is because the earlier the pursuer strategy switch occurs, the longer the defense team will use the wrong mode information. In contrast, the miss distance is not monotonically related to t_{sw} under the IMM strategy, but there is a t_{sw} corresponding to the maximum miss distance. Because the IMM strategy recognizes the pursuer's mode, an early pursuer switching strategy will leave the defending team more time to respond, while a late switching strategy will not allow enough time to boost the miss distance. Therefore, if the pursuer wants to break through the defender's defense it should switch its mode at the moment corresponding to the maximum miss distance. It can also be seen from the figure that when the defender's maximum acceleration is $1.3g$, and the pursuer completes the strategy switch before 13.3 seconds, the miss distance under the IMM strategy will be significantly lower than that of the CM strategy, and identifying the pursuer's strategy will lose its significance when $t_{sw} > 13.3$. When the defender's maximum acceleration is $1.5g$, switching modes before 14 s, the miss distance under the IMM strategy will be significantly lower than that under the CM strategy, and the maximum possible miss distance is much smaller.

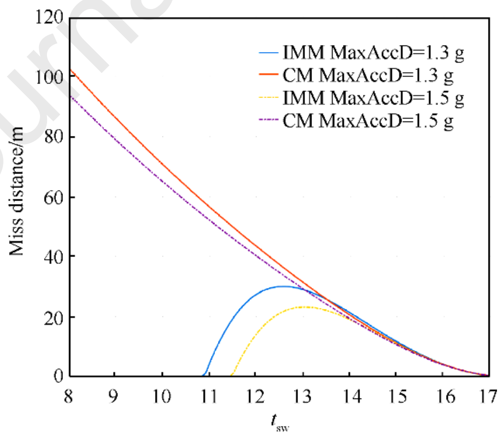

Fig. 12. Relationship between pursuer's strategy switch time and miss distance.

Subsequently, the performance of the cooperative guidance law designed in this study is analyzed using Monte Carlo simulations with 1000 samples. The initial values of each sample are randomly generated and the pursuer modes as well as the mode switch times in the samples are uniformly randomly selected. **Error! Reference source not found.** shows the CDF curves of the defending coalition adopting the strategy designed in this study under different defender's maximum acceleration. From the figure, it is evident that when the defender's maximum acceleration is 2*g*, about 98% of the samples' miss distance is less than 0.5 m. Therefore, the strategy designed in this study has a better interception performance when the pursuer can flexibly adjust its own mode. **Error! Reference source not found.** shows the CDF curves at different values of k_1, k_2 when the defense team adopts the CM strategy. From the figure, it can be observed that $(k_1 = 1, k_2 = 0), (k_1 = 0.2, k_2 = 0.8)$ performs the worst, while $(k_1 = 0.5, k_2 = 0.5)$ performs the best, which implies that adopting a mean strategy is a better choice when the pursuer pattern cannot be recognized.

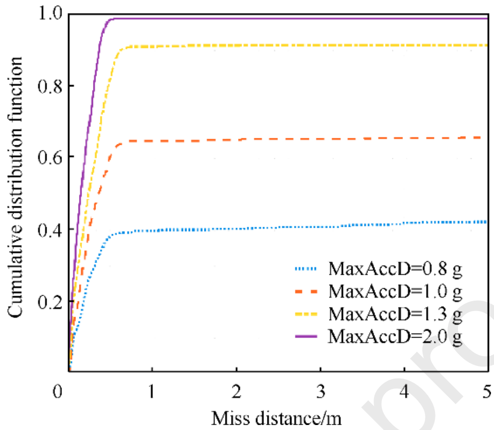

Fig. 19. CDF curves under the IMM strategy.

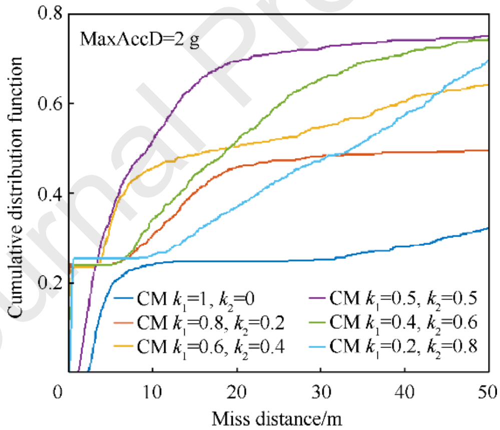

Fig. 20. CDF curves under the CM strategy.

Finally, we test the algorithm proposed in this paper under different orbital heights and different process noise covariance conditions. It also tests the calculation examples of 1000 random initial states and pursuer random switching strategies. **Error! Reference source not found.** shows the CDF curve of the IMM strategy at different orbital heights, and **Error! Reference source not found.** shows the CDF curve under the condition of different processes noise covariance. Q_1, Q_2, Q_3 are

$$
\begin{aligned}
Q_1 &= \mathrm{diag}\{6\times10^{-3}, 6\times10^{-3}, 6\times10^{-3}, 1\times10^{-3}, 1\times10^{-3}, 1\times10^{-3}\} \\
Q_2 &= \mathrm{diag}\{6\times10^{-3}, 6\times10^{-3}, 6\times10^{-3}, 1\times10^{-2}, 1\times10^{-2}, 1\times10^{-2}\} \\
Q_3 &= \mathrm{diag}\{6\times10^{-3}, 6\times10^{-3}, 6\times10^{-3}, 5\times10^{-2}, 5\times10^{-2}, 5\times10^{-2}\}
\end{aligned} \tag{55}
$$

As the height decreases, the condition $\|\delta \boldsymbol{r}\| / \|\boldsymbol{r}\| \ll 1$ is becoming more and more degraded, so the performance of the interception strategy based on the C-W equation will also deteriorate, but it can be seen from **Error! Reference source not found.** that the IMM strategy still meets the requirements in terms of interception performance. The covariance of process noise represents the degree of disturbance in the external environment. It can be seen from **Error! Reference source not found.** that under different covariance conditions, the IMM algorithm has good interception performance. Therefore, the IMM algorithm proposed in this paper has a certain robustness.

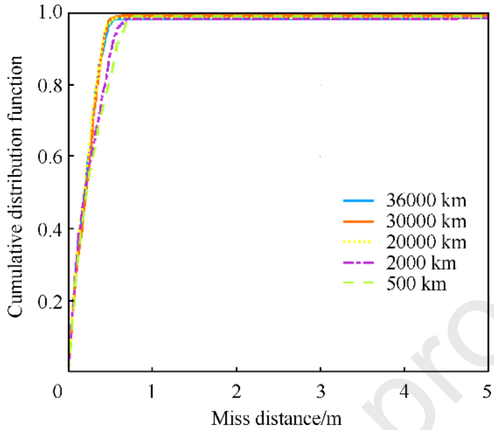

Fig. 21. CDF curve of IMM strategy at different virtual satellite heights.

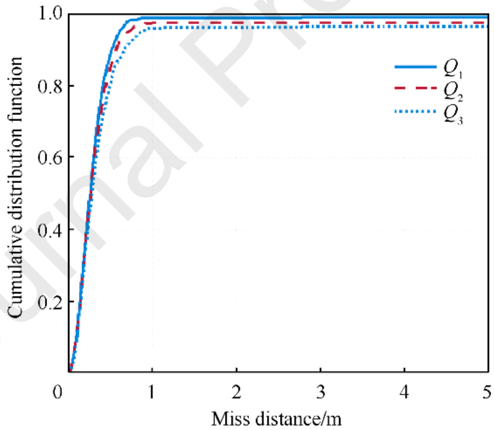

Fig. 22. CDF curve of IMM strategy under different process noise covariance conditions.

7. Conclusions

In this study, we design of a cooperative guidance law for evaders and defenders in an OPED. The pursuer's attack and avoidance modes are modeled based on the differential game theory for the characteristics of the pursuer who needs to capture the evader while bypassing the defender in the OPED. The attack mode is the most reasonable strategy that the pursuer can adopt when the pursuer does not have any further access to the evader's strategy. Similarly, when the pursuer has no further access to the defender's strategy, avoidance mode is the optimal strategy that it can play with the defender. Assuming that the pursuer will flexibly switch between attack and avoidance modes or flexibly adjust the weight between the two objectives of pursuing the evader and evading the defender during the game, the IMM-

SVSF algorithm was designed in this study to identify the pursuer's modes. Multiple parallel SVSFs match the different tendencies of the pursuer for each of the two targets, and the IMM updates the probabilities of the modes based on Bayesian inference. Combined with the results of the mode recognition, the two-way cooperative guidance law for the evader and defender was derived based on the optimal control theory.

The simulation results show that the IMM-SVSF algorithm has a good recognition of the pursuer's modes and a fast convergence speed for the pursuer's state estimation. The two-way cooperative guidance law based on mode recognition can significantly improve the interception performance against the pursuer. The focus of subsequent research will be to consider more complex game scenarios, such as situations where on-planet sensors have some type of constraint or where the external dynamic model is more complex. Scenarios in which there are multiple pursuers and defenders are also worth investigating, and the focus of this research will be on task allocation between defenders and pursuers.

Acknowledgements

The research leading to these results received funding from the Science and Technology Department, Heilongjiang Province under Grant Agreement No JJ2022LH0315.

References

[1] Fortunato, V. et al. A novel multi-mission platform for the development of applications, services, and new satellite data algorithms directly in orbit and on-demand, the Italian In-Orbit Space Lab. in 2023 European Data Handling & Data Processing Conference (EDHPC) 1–4 (IEEE, Juan Les Pins, France, 2023). doi:10.23919/EDHPC59100.2023.10396170.

[2] Hobbs, K. L., Davis, J., Wagner, L. & Feron, E. Formal Specification and Analysis of Spacecraft Collision Avoidance Run Time Assurance Requirements. in 2021 IEEE Aerospace Conference (50100) 1–16 (IEEE, Big Sky, MT, USA, 2021). doi:10.1109/AERO50100.2021.9438135.

[3] Bernhard, P., Deschamps, M. & Zaccour, G. Large satellite constellations and space debris: Exploratory analysis of strategic management of the space commons. Eur. J. Oper. Res. **304**, 1140–1157 (2023).

[4] Pontani, M. & Conway, B. A. Numerical Solution of the Three-Dimensional Orbital Pursuit-Evasion Game. J. Guid. Control Dyn. **32**, 474–487 (2009).

[5] Zeng, X., Yang, L., Zhu, Y. & Yang, F. Comparison of Two Optimal Guidance Methods for the Long-Distance Orbital Pursuit-Evasion Game. IEEE Trans. Aerosp. Electron. Syst. **57**, 521–539 (2021).

[6] Hafer, W. T., Reed, H. L., Turner, J. D. & Pham, K. Sensitivity Methods Applied to Orbital Pursuit

Evasion. J. Guid. Control Dyn. **38**, 1118–1126 (2015).

[7] Shi, M., Ye, D., Sun, Z., Zhong, W. & Deng, H. Spacecraft orbital pursuit–evasion games with J 2 perturbations and direction-constrained thrust. Acta Astronaut. **202**, 139–150 (2023).

[8] Ye, D., Shi, M. & Sun, Z. Satellite proximate pursuit-evasion game with different thrust configurations. Aerosp. Sci. Technol. **99**, 105715 (2020).

[9] Sun, S. et al. Numerical solution of a pursuit-evasion differential game involving two spacecraft in low earth orbit. J. Ind. Manag. Optim. **11**, 1127–1147 (2015).

[10] Shen, H.-X. & Casalino, L. Revisit of the Three-Dimensional Orbital Pursuit-Evasion Game. J. Guid. Control Dyn. **41**, 1823–1831 (2018).

[11] Li, Z., Zhu, H., Yang, Z. & Luo, Y. A dimension-reduction solution of free-time differential games for spacecraft pursuit-evasion. Acta Astronaut. **163**, 201–210 (2019).

[12] Zhang, J. et al. Near-optimal interception strategy for orbital pursuit-evasion using deep reinforcement learning. Acta Astronaut. **198**, 9–25 (2022).

[13] Ye, D., Shi, M. & Sun, Z. Satellite proximate interception vector guidance based on differential games. Chin. J. Aeronaut. **31**, 1352–1361 (2018).

[14] Tang, X., Ye, D., Huang, L., Sun, Z. & Sun, J. Pursuit-evasion game switching strategies for spacecraft with incomplete-information. Aerosp. Sci. Technol. **119**, 107112 (2021).

[15] Li, J., Li, C. & Zhang, Y. Guidance strategy of motion camouflage for spacecraft pursuit-evasion game. Chin. J. Aeronaut. S1000936123003515 (2023) doi:10.1016/j.cja.2023.10.007.

[16] Shen, D., Jia, B., Chen, G., Blasch, E. & Pham, K. Pursuit-evasion games with information uncertainties for elusive orbital maneuver and space object tracking. in (eds. Pham, K. D. & Chen, G.) 94690J (Baltimore, Maryland, United States, 2015). doi:10.1117/12.2181160.

[17] Comandur, V., Vechalapu, T. R., Makkapati, V. R., Tsiotras, P. & Hutchinson, S. Desensitization and Deception in Differential Games with Asymmetric Information. Dyn. Games Appl. (2024) doi:10.1007/s13235-024-00580-9.

[18] Asgharnia, A., Schwartz, H. M. & Atia, M. Deception In The Game of Guarding Multiple Territories: A Machine Learning Approach. in 2020 IEEE International Conference on Systems, Man, and Cybernetics (SMC) 381–388 (IEEE, Toronto, ON, Canada, 2020). doi:10.1109/SMC42975.2020.9283173.

[19] Vechalapu, T. R. A Trapping Pursuit Strategy for Capturing a High Speed Evader. in AIAA Scitech

2020 Forum (American Institute of Aeronautics and Astronautics, Orlando, FL, 2020). doi:10.2514/6.2020-2069.

[20] Shima, T. Optimal Cooperative Pursuit and Evasion Strategies Against a Homing Missile. J. Guid. Control Dyn. **34**, 414–425 (2011).

[21] Weiss, M., Shima, T., Castaneda, D. & Rusnak, I. Minimum Effort Intercept and Evasion Guidance Algorithms for Active Aircraft Defense. J. Guid. Control Dyn. **39**, 2297–2311 (2016).

[22] Perelman, A., Shima, T. & Rusnak, I. Cooperative Differential Games Strategies for Active Aircraft Protection from a Homing Missile. J. Guid. Control Dyn. **34**, 761–773 (2011).

[23] Li, C., Wang, J. & Huang, P. Optimal Cooperative Line-of-Sight Guidance for Defending a Guided Missile. Aerospace **9**, 232 (2022).

[24] Liang, H., Wang, J., Liu, J. & Liu, P. Guidance strategies for interceptor against active defense spacecraft in two-on-two engagement. Aerosp. Sci. Technol. **96**, 105529 (2020).

[25] Casbeer, D. W., Garcia, E. & Pachter, M. The Target Differential Game with Two Defenders. J. Intell. Robot. Syst. **89**, 87–106 (2018).

[26] Manoharan, A. & Baliyarasimhuni, S. Nonlinear Model Predictive Control Framework for Cooperative Three-Agent Target Defense Game. J. Intell. Robot. Syst. **108**, 21 (2023).

[27] Garcia, E., Casbeer, D. W. & Pachter, M. Design and Analysis of State-Feedback Optimal Strategies for the Differential Game of Active Defense. IEEE Trans. Autom. Control 1–1 (2018) doi:10.1109/TAC.2018.2828088.

[28] Pachter, M., Garcia, E. & Casbeer, D. W. Toward a Solution of the Active Target Defense Differential Game. Dyn. Games Appl. **9**, 165–216 (2019).

[29] Liang, L., Deng, F., Peng, Z., Li, X. & Zha, W. A differential game for cooperative target defense. Automatica **102**, 58–71 (2019).

[30] Liu, Y., Li, R., Hu, L. & Cai, Z. Optimal solution to orbital three-player defense problems using impulsive transfer. Soft Comput. **22**, 2921–2934 (2018).

[31] Zhou, J., Zhao, L., Cheng, J., Wang, S. & Wang, Y. Pursuer's Control Strategy for Orbital Pursuit-Evasion-Defense Game with Continuous Low Thrust Propulsion. Appl. Sci. **9**, 3190 (2019).

[32] Wei, Y., Liu, T., Wei, C., Zhang, R. & Gu, H. Two Hierarchical Guidance Laws of Pursuer in Orbital Pursuit–Evasion–Defense Game. Aerospace **10**, 668 (2023).

[33] Liang, L., Deng, F., Lu, M. & Chen, J. Analysis of Role Switch for Cooperative Target Defense

Differential Game. IEEE Trans. Autom. Control **66**, 902–909 (2021).

[34] Rubinsky, S. & Gutman, S. Three-Player Pursuit and Evasion Conflict. J. Guid. Control Dyn. **37**, 98–110 (2014).

[35] Rubinsky, S. & Gutman, S. Vector Guidance Approach to Three-Player Conflict in Exoatmospheric Interception. J. Guid. Control Dyn. **38**, 2270–2286 (2015).

[36] Zarchan, P. Tactical and Strategic Missile Guidance. (American Institute of Aeronautics and Astronautics, Reston, Va, 2007).

[37] Wang, S. B., Wang, S. C., Liu, Z. G., Zhang, S. & Guo, Y. Multi-agent cooperative multi-model adaptive guidance law. Aeronaut. J. **125**, 1103–1129 (2021).

[38] Habibi, S. The Smooth Variable Structure Filter. Proc. IEEE **95**, 1026–1059 (2007).

[39] Gadsden, S. A., El Sayed, M. & Habibi, S. R. Derivation of an optimal boundary layer width for the smooth variable structure filter. in Proceedings of the 2011 American Control Conference 4922–4927 (IEEE, San Francisco, CA, 2011). doi:10.1109/ACC.2011.5990970.

[40] Bar-Shalom, Y., Li, X.-R. & Kirubarajan, T. Estimation with Applications to Tracking and Navigation. (Wiley, New York, 2001).

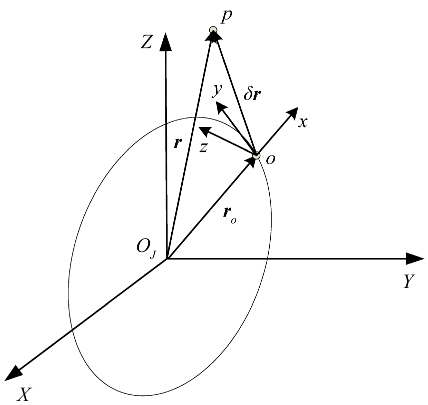
p
Z
y
δr
x
r
z
o
r_o
O_J
Y
X

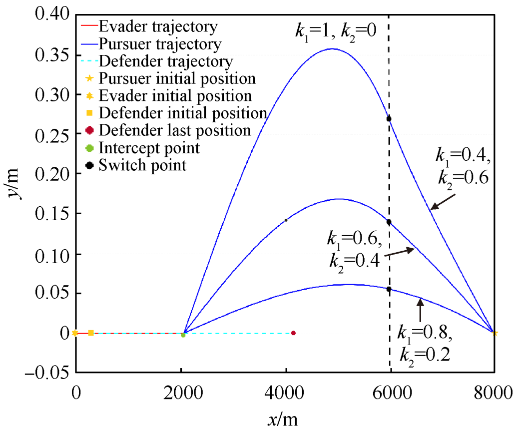
Evader trajectory
Pursuer trajectory
Defender trajectory
Pursuer initial position
Evader initial position
Defender initial position
Defender last position
Intercept point
Switch point
k_1=1, k_2=0
k_1=0.4, k_2=0.6
k_1=0.6, k_2=0.4
k_1=0.8, k_2=0.2
y/m
x/m
0.40
0.35
0.30
0.25
0.20
0.15
0.10
0.05
0
−0.05
0
2000
4000
6000
8000

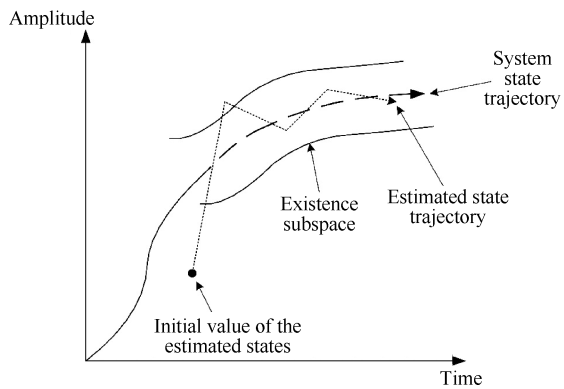
Amplitude
System
state
trajectory
Existence
subspace
Estimated state
trajectory
Initial value of the
estimated states
Time

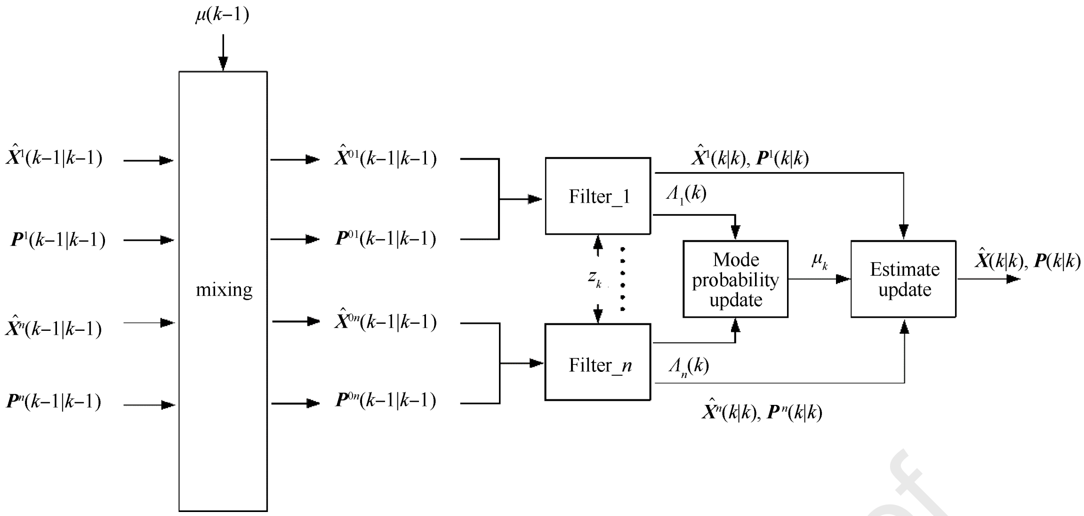

$\mu(k-1)$
mixing
$\hat{\boldsymbol{X}}^1(k-1|k-1)$
$\boldsymbol{P}^1(k-1|k-1)$
$\hat{\boldsymbol{X}}^n(k-1|k-1)$
$\boldsymbol{P}^n(k-1|k-1)$
$\hat{\boldsymbol{X}}^{01}(k-1|k-1)$
$\boldsymbol{P}^{01}(k-1|k-1)$
$\hat{\boldsymbol{X}}^{0n}(k-1|k-1)$
$\boldsymbol{P}^{0n}(k-1|k-1)$
Filter_1
Filter_n
z_k
$\hat{\boldsymbol{X}}^1(k|k)$, $\boldsymbol{P}^1(k|k)$
$\Lambda_1(k)$
Mode probability update
μ_k
Estimate update
$\hat{\boldsymbol{X}}(k|k)$, $\boldsymbol{P}(k|k)$
$\Lambda_n(k)$
$\hat{\boldsymbol{X}}^n(k|k)$, $\boldsymbol{P}^n(k|k)$

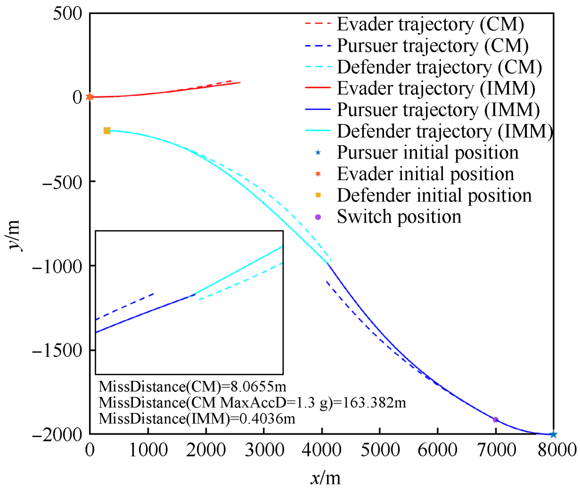
Evader trajectory (CM)
Pursuer trajectory (CM)
Defender trajectory (CM)
Evader trajectory (IMM)
Pursuer trajectory (IMM)
Defender trajectory (IMM)
Pursuer initial position
Evader initial position
Defender initial position
Switch position
MissDistance(CM)=8.0655m
MissDistance(CM MaxAccD=1.3 g)=163.382m
MissDistance(IMM)=0.4036m
y/m
x/m
500
0
−500
−1000
−1500
−2000
0
1000
2000
3000
4000
5000
6000
7000
8000

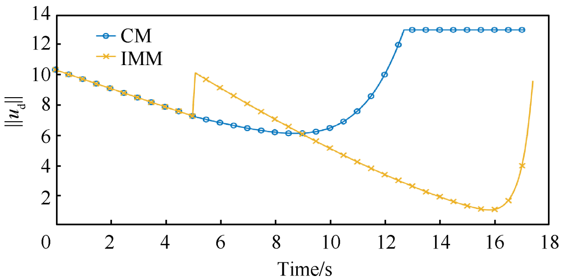
CM
IMM
$\|u_d\|$
Time/s
0
2
4
6
8
10
12
14
16
18

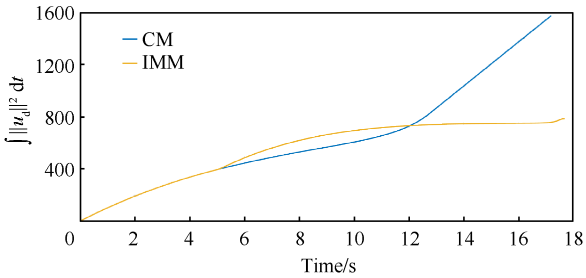

1600
1200
800
400
0
2
4
6
8
10
12
14
16
18
Time/s
$\int \|u_d\|^2\, dt$
CM
IMM

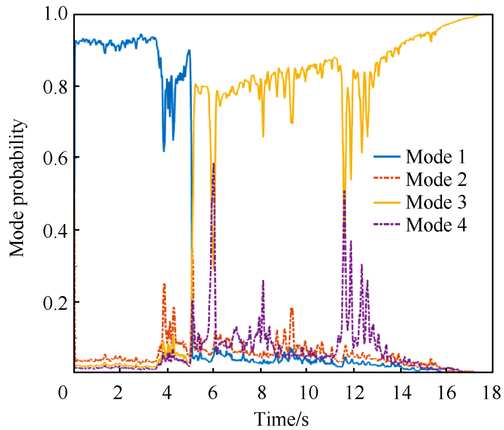
1.0
0.8
0.6
0.4
0.2
0
2
4
6
8
10
12
14
16
18
Mode probability
Time/s
Mode 1
Mode 2
Mode 3
Mode 4

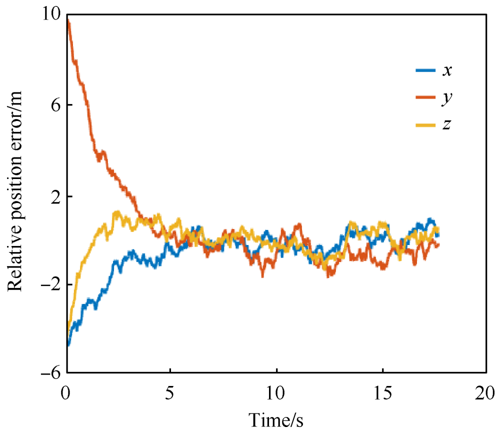
10
6
2
−2
−6
0
5
10
15
20
Time/s
Relative position error/m
x
y
z

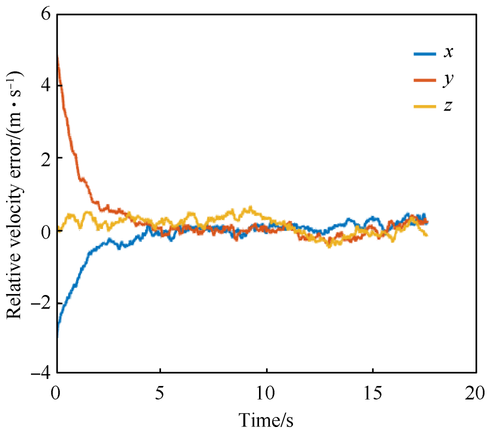
6
4
2
0
−2
−4
0
5
10
15
20
Time/s
Relative velocity error/(m • s⁻¹)
x
y
z

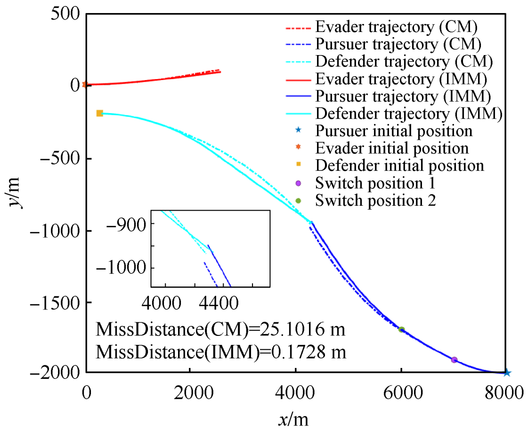

Evader trajectory (CM)
Pursuer trajectory (CM)
Defender trajectory (CM)
Evader trajectory (IMM)
Pursuer trajectory (IMM)
Defender trajectory (IMM)
Pursuer initial position
Evader initial position
Defender initial position
Switch position 1
Switch position 2
MissDistance(CM)=25.1016 m
MissDistance(IMM)=0.1728 m
y/m
x/m
500
0
−500
−1000
−1500
−2000
2000
4000
6000
8000
−900
−1000
4000
4400

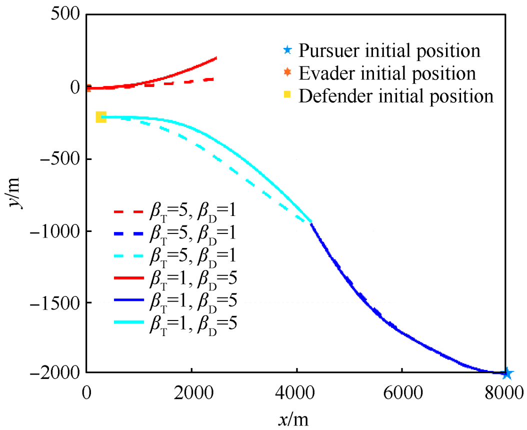
500
0
−500
−1000
−1500
−2000
0
2000
4000
6000
8000
x/m
y/m
Pursuer initial position
Evader initial position
Defender initial position
βT=5, βD=1
βT=5, βD=1
βT=5, βD=1
βT=1, βD=5
βT=1, βD=5
βT=1, βD=5

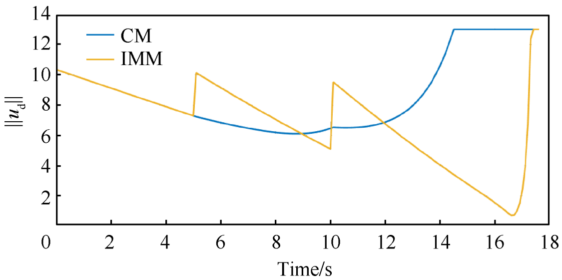

CM
IMM
14
12
10
8
6
4
2
0
2
4
6
8
10
12
14
16
18
$\|u_d\|$
Time/s

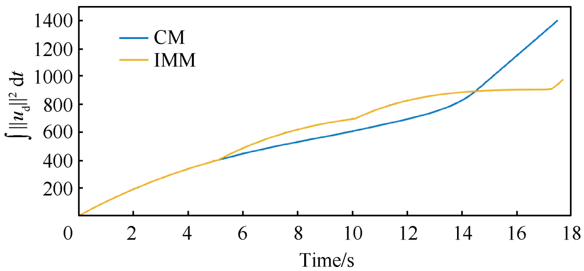
CM
IMM
1400
1200
1000
800
600
400
200
0
2
4
6
8
10
12
14
16
18
Time/s

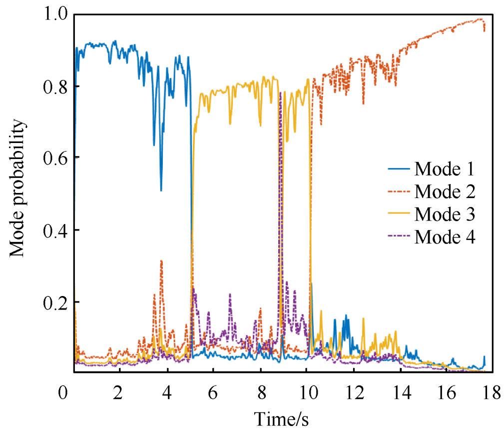
1.0
0.8
0.6
0.4
0.2
Mode probability
0
2
4
6
8
10
12
14
16
18
Time/s
Mode 1
Mode 2
Mode 3
Mode 4

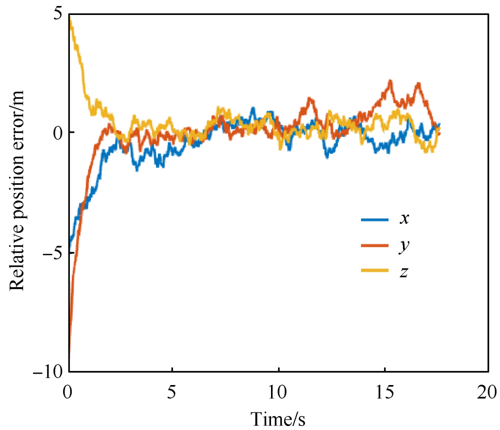

Relative position error/m
5
0
−5
−10
0
5
10
15
20
Time/s
x
y
z

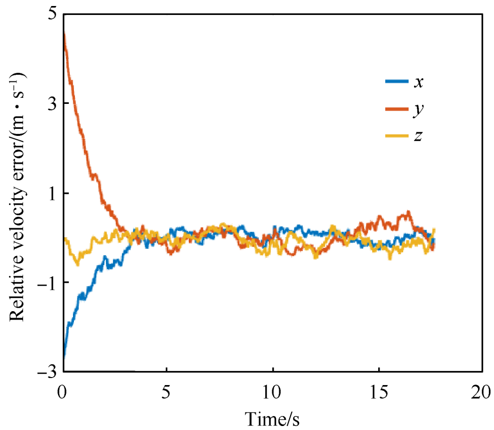

5
3
1
−1
−3
0
5
10
15
20
Relative velocity error/(m · s⁻¹)
Time/s
x
y
z

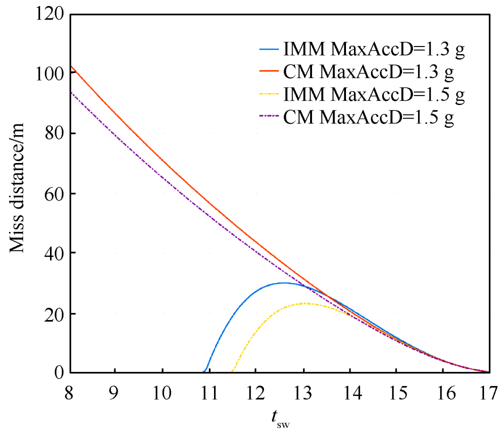

IMM MaxAccD=1.3 g
CM MaxAccD=1.3 g
IMM MaxAccD=1.5 g
CM MaxAccD=1.5 g
Miss distance/m
t_{sw}
0
20
40
60
80
100
120
8
9
10
11
12
13
14
15
16
17

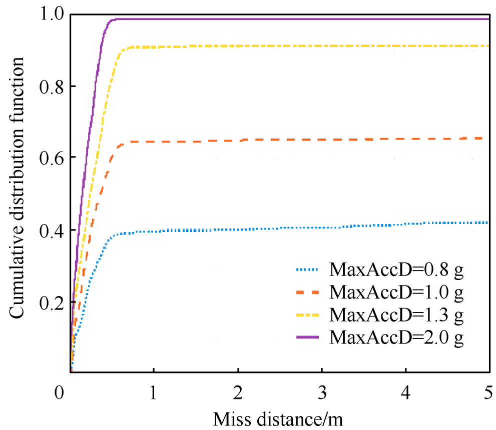
1.0
0.8
0.6
0.4
0.2
0
1
2
3
4
5
Cumulative distribution function
Miss distance/m
MaxAccD=0.8 g
MaxAccD=1.0 g
MaxAccD=1.3 g
MaxAccD=2.0 g

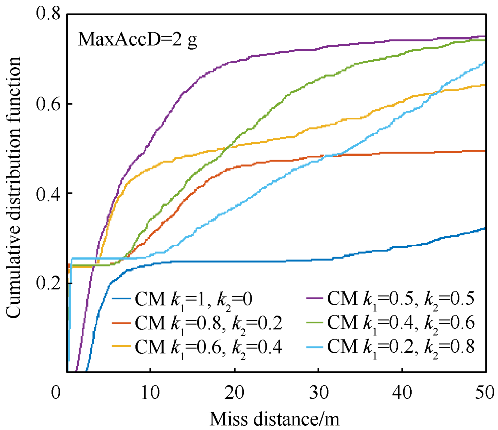
MaxAccD=2 g
Cumulative distribution function
Miss distance/m
0.8
0.6
0.4
0.2
0
10
20
30
40
50
CM k_1=1, k_2=0
CM k_1=0.8, k_2=0.2
CM k_1=0.6, k_2=0.4
CM k_1=0.5, k_2=0.5
CM k_1=0.4, k_2=0.6
CM k_1=0.2, k_2=0.8

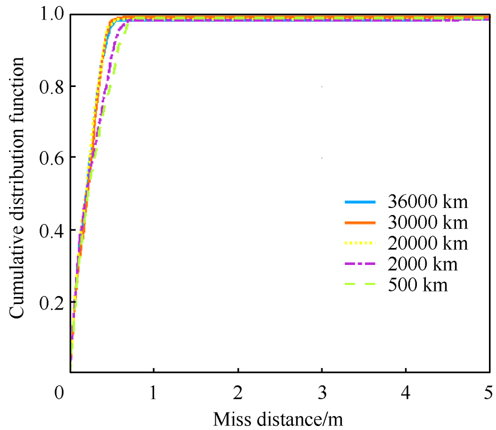

1.0
0.8
0.6
0.4
0.2
Cumulative distribution function
36000 km
30000 km
20000 km
2000 km
500 km
0
1
2
3
4
5
Miss distance/m

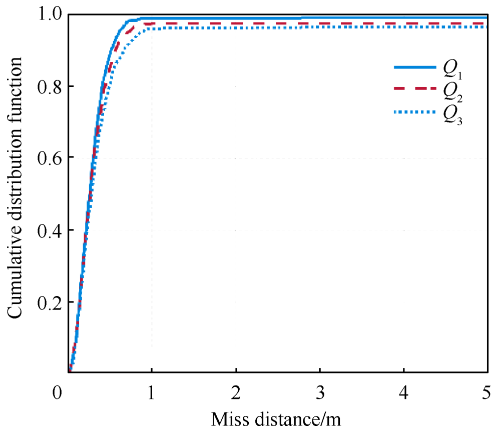
1.0
0.8
0.6
0.4
0.2
0
1
2
3
4
5
Cumulative distribution function
Miss distance/m
Q_1
Q_2
Q_3

Highlights

• Depending on the pursuer's control objective in the orbit pursuit-evasion defense scenario, its behavioral modes are modeled according to differential game theory and divided into an attack mode against evader maneuvers and an avoidance mode against defender maneuvers.

• In response to the different behavioral patterns of the pursuer, a two-way cooperative optimal guidance law for the evader and defender is derived based on optimal control theory, which reduces the miss distance and control effort of the defender through cooperation between the evader and defender.

• A mode recognition algorithm with a joint interactive multiple model and smooth variable structure filtering is proposed to recognize the pursuer's intention through historical observation information, thereby executing the collaborative strategy in the corresponding mode.

Declaration of interests

☒ The authors declare that they have no known competing financial interests or personal relationships that could have appeared to influence the work reported in this paper.

☐ The author is an Editorial Board Member/Editor-in-Chief/Associate Editor/Guest Editor for *[Journal name]* and was not involved in the editorial review or the decision to publish this article.

☐ The authors declare the following financial interests/personal relationships which may be considered as potential competing interests: